8-8-2007

A New Method to Predict Vessel Capsizing in a Realistic Seaway

Srinivas Vishnubhotla
University of New Orleans

A New Method to Predict Vessel Capsizing in a Realistic Seaway

A Dissertation

Submitted to the Graduate Faculty of the
The University of New Orleans
in partial fulfillment of the
requirements for the degree of

Doctor of Philosophy
in
Engineering and Applied Science
Naval Architecture and Marine Engineering

by

Srinivas Vishnubhotla

B.S., Indian Institute of Technology, Kharagpur, India, 1993
M.S., University of New Orleans, New Orleans, USA, 1998

August 2007

DEDICATION

Dedicated to my mother Indira Vishnubhotla, my father Venkatratnam Vishnubhotla for supporting me throughout my education and my brother Vijaykumar Vishnubhotla for always encouraging me.

ACKNOWLEDGEMENT

Completing this doctoral work has been a wonderful and often overwhelming experience. It is hard to know whether it has been grappling with understanding the physics of ship motions itself which has been the real learning experience, or grappling with how to write a paper, give a coherent talk, work in a group, teach section, code intelligibly, recover a crashed hard drive, stay up until the birds start singing, and... stay, um... focussed.

I have been very privileged to have undoubtedly the most intuitive, smart and supportive advisor anyone could ask for, namely Dr. Jeffrey M. Falzarano. He has fostered certainly the most open, friendly, collaborative and least competitive research group over the years that I have known him in this school of Naval Architecture and Marine Engineering (NAME) program. He has also known when (and how) to give me a little push in the forward direction when I needed it.

I was supported for many semesters of course work and research work by the University of New Orleans' Crescent City Doctoral Scholarship, by Office of Naval Research (ONR) and Gulf Coast Region Maritime Technology Center (GCRMTC) sponsored projects through the generosity of my advisor.

My sincere thanks to Dr. Alexander Vakakis for introducing us to his unique mathematical approach, without whom this thesis would not have been possible in the first place, and guiding me throughout when we (I or Dr. Falzarano) needed his assistance. Dr. Falzarano's other students, both past and present, comprised a superb research group. The ability to bounce ideas off so many excellent minds has been priceless. I would also like to thank the members of my dissertation committee for their invaluable suggestions and advice during the final stages of my defense.

During my graduate studies of fulfilling my course work requirements, besides Dr. Falzarano, I am very much indebted to the knowledge gained in taking courses from Dr. William Vorus (current Chairman of NAME) whose clarity, persistence for quality and his ability to set high standards (and challenging tests!) has been a great learning curve. Courses from other distinguished professors in other Engineering and Science departments such as Dr. Kazim Akyuzlu, Dr. Lew Lefton, Dr. Stephen Lipp, Dr. William St. Cyr., Dr. Robert Fithen and Dr. Martin Guillot also has taught me a lot.

I like to thank Dr. Lothar Birk for introducing me to Latex in my final stages of thesis formatting challenges. It has been my pleasure to know and work with George Morrissey, who has always been helpful to me.

Thanks also go to my friends Rangel Vassilev (my colleague in school and my housemate 'pre-Katrina'), Charles Walton, Sandor Kelemen, Angela Marchese and Kathy Brou for being there during the difficult times before and after 'Katrina'.

A special thanks to my new dear friend, Rachel Stevenson, for supporting me always and making me smile since we got acquainted. For my tango mentors Susana Miller and Joan Bishop, for all the encouragement and support.

I owe my childhood education entirely to my parents and my brother - my courageous mother who didn't flinch to guide me through to the right opportunities; my father for expanding my general awareness and being my hero while also enhancing my interest in music and introducing me very early to childrens' literature in the form of 'Indrajal' comic books of India (that I still read to this day); my brother who kept my interest for physics alive and for all the love and encouragement he has given while treating me like his own son.

CONTENTS

LIST OF FIGURES

LIST OF TABLES

ABSTRACT

A recently developed approach, in the area of nonlinear oscillations, is used to analyze the single degree of freedom equation of motion of a floating unit (such as a ship) about a critical axis (such as roll). This method makes use of a closed form analytic solution, exact upto the first order, and takes into account the the complete unperturbed (no damping or forcing) dynamics. Using this method very-large-amplitude nonlinear vessel motion in a random seaway can be analysed with techniques similar to those used to analyse nonlinear vessel motions in a regular (periodic) or random seaway. The practical result being that dynamic capsizing studies can be undertaken considering the short-term irregularity of the design seaway. The capsize risk associated with operation in a given sea state can be evaluated during the design stage or when an operating area change is being considered. Moreover, this technique can also be used to guide physical model tests or computer simulation studies to focus on critical vessel and environmental conditions which may result in dangerously large motion amplitudes. Extensive comparitive results are included to demonstrate the practical usefulness of this approach. The results are in the form of solution orbits which lie in the stable or unstable manifolds and are then projected onto the phase plane. [1]

[1] keywords: nonlinear ship/platform motions; ship capsize; dynamical perturbation; random beam seas; large amplitude ship rolling; stable and unstable manifolds.

1. INTRODUCTION

1.1 Background and Motivation

One of the many challenges facing ship and floating offshore structures design today is the survivability to not capsize under adverse if not the most extreme weather conditions. The external forces acting on the hull are to a large extent those from wind, waves and current. The prevailing tools of the past enabled the naval architect to analyze ship stability based solely on hydrostatics where the restoring ability of the unit is assessed due to steady wind alone and the motion response of the unit was investigated considering only linear dynamics (using only the linear damping and restoring terms in the roll equation of motion) and periodic forcing due to regular waves. When a floating vessel is subjected to an external forcing such as that due to wave excitation, the vessel may capsize due to a number of factors depending on the magnitude and direction of the wave excitation and the unit's resistance to the given excitation. One of the modes of motion identified among the statistical survey of capsized units has been the 'roll' mode when large waves were seen to approach the ship from the side ("beam seas") or at some times along an oblique direction in some cases for a 'column stabilized' unit such as a floating platform.

The only form of appreciable resistance offered by the unit in such modes which are typically resonant in nature is through the so called reactive 'damping' forces which are generally very small in order of magnitude compared to the other forces like restoring. This results in large amplitude response of the unit which requires consideration of non-linear statics and to some extent non-linear dynamics since part of the damping reaction force is due to 'viscous' damping, a quantity not easy to estimate. It has been predicted that vessel capsizing in realistic waves is associated with large amplitude dynamic phenomena requiring consideration of non-linear and probabilistic dynamics. Also advances in topics related to large amplitude oscillation and non-linear dynamics have suggested that the traditional ship stability approach is very limited in predicting a floating

units ability to resist capsize, especially when the dominant forces are due to waves from random seas (Falzarano, 1990).

The problem of predicting the roll response of ships and the response about a critical axis for other floating structures has been a subject of wide interest, concern and challenge in the last two decades owing to a staggering number of ships, fishing and/or crabbing vessels and other offshore platforms lost at sea. Although vessel capsizing is now well understood to be a large amplitude dynamic phenomenon, the ability to accurately assess the conditions under which the unit is susceptible to be unsafe is challenging and still an on-going research topic especially when the forcing function is considered to be random or irregular which is the case due to a realistic seaway. However it is suggestive and insightful to review the studies undertaken by research groups, scientists and engineers in the recent past who have attempted to understand and relate the ship rolling as a vibration phenomenon exhibiting non-linear resonance characteristics such as chaos under certain conditions and eventually leading to loss of dynamic stability and/or capsize.

1.2 Related Studies

The non-linear roll response of ships to irregular random excitation, although without an emphasis on capsize risk, has been addressed as early as in 1964 by Hasselman, Yamanuchi and others. Hasselman (1965) considered the complete six degrees of freedom ship motion response and showed that the non-linear transfer functions are related to the higher order moments of the ship motions due to a (pseudo) random stationary wave field approximated by a Fourier sum. For the uncoupled non-linear roll equation of motion excited by a white noise, Yamanouchi (1986) used a perturbation method using a small parameter measuring the extent of non-linearity in stiffness to estimate the variance of roll and roll velocity approximate up to the first order. Using a similar technique whereby expressing the solution to the roll equation as a Volterra series for the same problem, Flower (1975) observed that the non-linearity had an effect of hardening the roll spectrum obtained from a linear analysis. Alternatively the technique of equivalent linearization was well explored by Vassilopoulos (1971) where non-linearity was included in both stiffness (cubic) and damping (square law) and the results for the variance of roll and roll velocity compared well with the previous (perturbational) approaches.

The nonlinear roll response of ships to regular periodic wave excitation was studied by a number of research groups beginning with Cardo and Francescutto (1982) who observed a variety of interesting phenomena including ultra-harmonics and sub-harmonics in the steady state solutions. Capsize criteria based on a certain safety factor was proposed by Virgin (1987) while observing the chaotic dynamics of the single degree of freedom roll equation of motion with and without a static bias. Numerical simulation techniques and analytical solutions using a harmonic balance method were utilized by considering quadratic and cubic nonlinearity to the restoring force in the equation of motion. Nayfeh et.al (1986) did an independent study of the nonlinear rolling of ships with and without bias due to regular beam seas. Using the method of multiple scales and comparing with numerical simulations they showed that the second order perturbation expansion was more accurate than the first order in predicting the peak roll angle and the start of the period multiplying bifurcations that lead to chaos.

Thompson (1990, 1997), Soliman et. al. (1990) and more recently Huang (2000, 2003) generalized the problem of capsize to that of the escape from a potential well through the representation of bifurcation and integrity maps and studied the erosion of safe basin for both steady state and transient motions. Roberts (1995) addressed the problem of non-linear ship rolling in random beam seas by the use of statistical linearization and Fokker-Plank equation techniques to study the stochastic roll response and demonstrate the existence of bifurcation phenomena leading to chaos. Highlighting the importance of narrowbanded Gaussian or non-gaussian stochastic excitation of a short term sea spectra, Francescutto (1993) used Fokker-Planck equation technique to demonstrate the existence of bifurcation phenomena leading to chaos similar to the corresponding deterministic counterpart. It is further noted that the possibility of observing bifurcations and other related phenomena is cancelled if the bandwidth is not narrowbanded without ensuring that they cannot be realized, which can be critical in the estimation of the probability of vessel capsize.

Roberts (1986, 1998) discussed the problem of ship rolling in random beam seas due to stationary stochastic excitation where non-linearity in both damping and restoring moment was adopted. For moderate rolling, statistics of the stochastic roll response is developed using both equivalent linearization method and Markov process theory. For severe rolling, first passage statistics such as mean time to capsize are computed using the Markov approximation. The theory is also extended into an assessment of long-term roll statistics.

One of the methods also employed extensively by research groups and scientists in the recent past in considering the non-linear behavior of a ship system was by the use of dynamical systems approach to either a single degree of freedom or coupled ship motion equations through the use of analytical or numerical solution techniques (Frey & Simiu, Lin & Yim, Falzarano, Jiang & Hsieh). Frey and Simiu (1993, 1996) developed a theoretical basis for weak perturbations (both periodic and quasi periodic forcing) and the effect of noise on second order dynamical systems whose unperturbed flows have homoclinic or heteroclinic orbits. They justified in applying and formulating a more generalized Melnikov treatment for stochastic perturbations by conforming the noise to a harmonic sum with random parameters whose paths are uniformly bounded. The flux factor for the phase space is derived and shown that the mean distribution of the filtered excitation determines the average phase space flux. One of the important conclusions drawn for the dynamical systems considered is that the two classes of excitation namely, stochastic and deterministic, are equivalent in the promotion of chaos and in reducing the safe basin of the system.

Lin and Yim (1996, 2004) examined the noise induced periodic, chaotic and capsizing responses of a ships roll motion and the associated extreme value distribution. Using a generalized Melnikov function as proposed by Frey and Simiu (1993, 1996), an upper bound for possible chaotic motion is established within the control space of the parameters and it is shown that noise could lower the threshold for chaotic ship roll motion. The transition between purely periodic, chaotic or non-chaotic random to purely random responses are investigated by solving the associated Fokker-Planck equation governing the evolution of the probability density function (PDF) of the roll motion. It is further shown for the heteroclinic chaotic motions that the probability of extreme excursions is elevated with increasing noise intensity, which increases the probability of capsize.

Hsieh et.al (1994) and Jiang et.al (1996) investigated the capsize criteria for unbiased and biased ships respectively due to a pseudo random excitation. Again using the generalized Melnikov function as developed by Frey and Simiu, the rate of phase space flux due to random excitation such as due to a realistic sea state is examined and the probability of capsize is predicted. Unlike the previous studies which used constant values for the linear added mass and damping coefficients, Jiang et.al (1996, 2000) incorporated the frequency dependence of the linear hydrodynamic force coefficients due to the presence of free surface. This was done with the help of convolution integral to capture the radiated wave force effects in the form of an integro-differential equation in the time

domain.

Successful use of modern geometric methods in considering the ship dynamical system, which usually focus on the nature and evolution of global unperturbed solution or orbit trajectories to small perturbations in forcing and/or damping, and numerical simulations of the exact or approximate solutions at least due to periodic forcing of the complete system of non-linear equations of ship/platform motions has, to a greater extent, highlighted the significance of the solution behavior and its influence on the floating units stability. In the proposed thesis, similar methods are extended to understand the dynamical stability of such units under realistic/random forcing function such as those arising due to a design seaway from a short term distribution of wave energy.

Some of the recent and existing methods focus in predicting the safe or non-capsize boundary of a floating unit by extending the Melnikov approach and studying phase space transport in a probabilistic sense due to a pseudo random excitation. The Melnikov technique (Melnikov, 1962) is essentially an extension of the modern geometric method in problems associated with nonlinear oscillations, where the distance between the stable and unstable solutions or orbits lying on their respective manifolds (a collection or family of such solutions which are invariant in time) is determined from the known unperturbed solutions. Global bifurcations leading to chaos are then predicted based on this distance between manifolds becoming zero or positive. Equivalently, from a physical point of view, the Melnikov function represents the difference in the work done by the forcing or excitation and the energy exhausted due to the systems damping (Er, G-K et.al, 1999, 2000). The strength or the effectiveness of the standard Melnikov approach lies in not needing to know the exact or approximate solution under the effect of small forcing and damping yet being able to predict the onset of capsizing if the system solution is known in its unperturbed state. Numerical techniques when the forcing is periodic have been utilized to predict the safe basin boundaries once the periodic orbits or the saddle point equilibrium points of the corresponding Poincaré map are located. Determination of the equilibrium points and the basin boundaries by this approach without the full knowledge of the stable/unstable manifolds is usually time consuming and not always straightforward especially when the forcing function is at or above a certain threshold value.

More recently an approach first investigated for periodic excitation by Vakakis (1993) and applied extensively to the well known Duffing oscillator problems involving homoclinic connections

concentrates on exploring a closed form solution to the stable and unstable manifolds up to the first order of approximation. The focus of the method utilized in the current work is the application of the so-called Vakakis approach to floating units (both ship shape and any other floating offshore platform units) under a realistic/random forcing function. The angles of vanishing stability in the critical modes of motion (usually the transverse or the roll axis for a ship shape body and a diagonal axis for a semi-submersible) are closely related to the heteroclinic connections of the manifolds under non-linear restoring, small damping and forcing respectively. The measure of the distance between the manifolds can then be computed directly from the known first order solutions. This is compared with the Melnikov method, which doesn't require the solution of the perturbed manifolds, as applied in the previous studies for a similar problem (Hsieh et.al, 1993).

The approximate (Melnikov) distance function between the manifolds is linearly dependent on the excitation amplitude and in a complicated way on the excitation frequency. For the periodic case, given an amplitude and excitation frequency, it has been also shown that the distance function depends on the phase of the excitation relative to the forcing frequency and it has been an exercise of previous studies to determine at what phase (or at what initial time) does the Melnikov function attain simple zeroes. The existence of zeroes in the distance function such as that approximated by the Melnikov function implies that the phase space contains heteroclinic tangles giving rise to global bifurcation phenomenon often leading to complicated dynamics (Wiggins, 1990). One consequence of this situation is that the dynamics of the system started near the angle of vanishing stability are now essentially unpredictable (even under periodic deterministic excitation) resulting in aperiodic response and at times leading to unexpected capsize (Falzarano, 1990). Another effect of these zeroes is that the net area of the lobes (phase space flux in and out of an imaginary boundary called the pseudo-separatrix) as approximated by the Melnikov function which is positive is related to the amount of phase space transported out of the 'safe region'.

A major thrust of the current thesis will be to observe how the above findings differ or are similar under irregular forcing such that due to a pseudo random excitation model which is realistically based on a 'long-crested' (unidirectional) sea developed from a given short-term sea state description usually characterized by a period and a significant wave height. Part of the inspiration for the current endeavor stems from other related works such as those by Frey and Simiu (1993) and Hsieh et. al. (1994) who extended the phase space transport theory developed for

periodic systems to multi-harmonic excitations. There is also a motivation to apply the perturbed solutions approach up to the first order (Vakakis, 1993) as it relates to the ship dynamical problem (with no initial static bias) and to study the extension of this approach under irregular forcing. As a first exercise the perturbed stable and unstable solutions are computed and then calculated as a function of the system parameters and the external excitation.

Since much of the focus is on whether or not a given vessel will capsize under a given excitation level, the relation between the manifold intersections and the phase space transport dynamics is re-visited for a pseudo random excitation. Specifically the distance function with the known perturbed solutions is compared with the Melnikov techniques as explained by previous studies to see if we learn anything more or if we can better approximate the separation distance between the manifolds. Also while most of the current work herein assumes constant added mass and damping coefficients in determining the system parameters of the roll equation of motion, an effort has also been included to incorporate a more accurate modeling with respect to the memory-dependent hydrodynamics for the linear radiated wave force damping especially since the excitation is a pseudo random forcing consisting of a large number of input frequencies. This accommodates the use of frequency dependent coefficients since we know that the added mass and the damping coefficients are only constant if the forcing is harmonic at a singe frequency and the system is linear.

1.3 Summary of Chapters

The formulation of the thesis is divided into four main chapters. The second chapter details the mathematical formulation of the ship dynamics problem as it applies to the roll mode in isolation from other degrees of freedom. The third chapter is devoted to the use of a dynamical systems approach to obtain certain specific solutions of the highly nonlinear roll equation of motion under random excitation. The solution procedure as well as the use of the perturbed solutions as it relates to vessel capsize is explored and compared with some recent studies to understand the nonlinear and transient nature of the ship/vessel dynamics due to large amplitude random wave excitation. The fourth chapter applies the methodology developed in previous chapters to obtain results for some specific vessel types and justifies the significance of the approach developed herein as it relates to other methodologies and other available simulation based approaches. Based on understanding

the assumptions and approximations made in applying the current method, a discussion for future work and improvements in approximation are also suggested in the final chapter five.

2. FORMULATION OF SHIP ROLL EQUATION OF MOTION

2.1 Reference frames and rigid body motions

It is common in the seakeeping theory to use either an earth fixed (inertial) coordinate system or a body-fixed system to describe the motion of the fluid or of the floating unit in the fluid. Depending on the problem to be solved at hand it is customary to choose one system over the other, though it is always necessary to then relate the two systems using coordinate transformations (either angles or translations) especially when dealing with finite displacements. A body fixed orthogonal right hand axis system, with origin at the mid-ship and design waterline, is chosen as shown in Figure 2.1. (u, v, w) is the velocity vector of the translational motions surge, sway and pitch; (p, q, r) is the angular velocity vector of the rotational motion roll, pitch and yaw. The nonlinear coupled rigid body equations of motion (obtained from the general theory of rigid body motions or Newtons Laws) with origin not at the center of gravity are called Eulers equations of motion. These equations

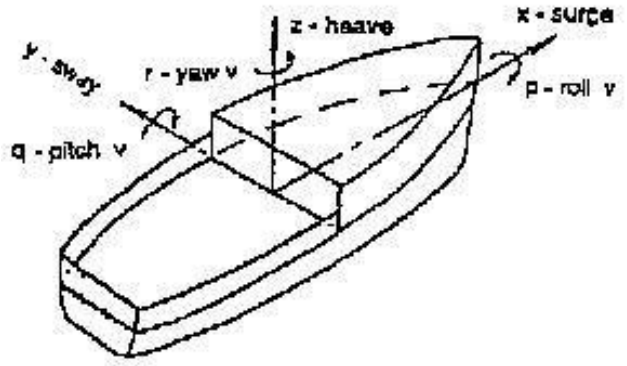

Fig. 2.1: Ship coordinate system

are derived or reported in a variety of references (see e.g., Falzarano, 1990), as shown in (2.1)

$$
\begin{aligned}
X &= m[\dot{u} + qw - rv - x_G(q^2 + r^2) + z_G(pr + \dot{q})] \\
Y &= m[\dot{v} + ru - pw - x_G(pq + \dot{r}) + z_G(qr - \dot{p})] \\
Z &= m[\dot{w} + pv - qu + x_G(rp - \dot{q}) - z_G(p^2 + q^2)] \\
K &= I_{44}\dot{p} - (I_{55} - I_{66})qr - I_{64}(\dot{r} + pq) - mz_G(\dot{v} + ru - pw) \\
M &= I_{55}\dot{q} - (I_{66} - I_{44})rp - I_{64}(r^2 - p^2) + mz_G(\dot{u} + qw - rv) - mx_G(\dot{w} + pv - qu) \\
N &= I_{66}\dot{r} - (I_{44} - I_{55})pq - I_{64}(\dot{p} - qr) + mx_G(\dot{v} + ru - pw)
\end{aligned}
\tag{2.1}
$$

where m is the mass of the ship, I_{44}, I_{55}, I_{66} and I_{64} are the moments of inertia.

(X,Y,Z) is the force vector and (K,M,N) is the moment vector which are defined in the body-fixed coordinate system. The force (and the moment) vector represent the generalized hydrodynamic forces (and moments) for the six degrees of freedom expressed in the body fixed system. The total hydrodynamic force vector is assumed to be broadly a combination of:

a) the wave excitation force comprising of two components namely *Froude-Krilov* forces which are due to the incident wave in the assumption that the presence of the hull does not alter the flow field and *diffraction* forces which consider the effect of change in the flow field due to the fluid structure interaction;

b) the radiation forces which appear as a consequence of the change in momentum of the fluid and the waves generated due to the motion of the hull. These forces are proportional to the accelerations and velocities of the vessel and hence the radiation forces are separated into the so-called *added-mass* forces (forces proportional to accelerations) and *potential-damping* forces (forces proportional to velocities);

c) the viscous forces which are nonlinear damping forces that appear due to viscous effects such as skin friction, flow separation, eddy making etc. These forces depend nonlinearly on the relative velocities between the hull and the fluid;

d) the hydrostatic forces which are the restoring forces due to gravity and buoyancy that tend to preserve the equilibrium of the vessel. There could be other external forces due to wind, current and other effects (such as water on deck, thrusters, mooring etc) that are ignored for the

current thesis which focuses chiefly on the response of the floating unit due to gravity waves alone. Similarly there could be external forces due to the constant forward speed of the unit and the waves which are usually the result of the so-called second order effects and these are again ignored for the current study herein. This is found acceptable if the forward speed on the unit is generally small.

Except for the viscous forces the rest can be studied within a linear frame-work. In particular the wave excitation forces and the radiation forces can be obtained by considering the linear potential theory where a potential function that satisfies the Laplace's Equation (see equation (2.2) or e.g., Chakrabarti, (1997)) in the fluid and boundary conditions on the surface of the hull, the free surface of the water and the sea floor.

$$\nabla^2\Phi = 0 \tag{2.2}$$

Due to linearity, this potential is separated into radiation potential and wave-excitation potential. The pressure can be calculated by substituting the potential into the linearized Bernoulli Equation (2.3).

$$\frac{p}{\rho} + \frac{\partial\Phi}{\partial t} + gz = C \tag{2.3}$$

and the hydrodynamic forces and moments are obtained by integrating the pressure over the wetted surface S_w of the hull. The radiation components thus for each degree of freedom are given by:

$$F_{ri} = -\rho \iint_{S_w} (\tfrac{\partial\Phi_r}{\partial t} + gz)(n)_i ds \quad i = 1,2,3 \tag{2.4}$$

$$F_{ri} = -\rho \iint_{S_w} (\tfrac{\partial\Phi_r}{\partial t} + gz)(r \times n)_i ds \quad i = 4,5,6 \tag{2.5}$$

Similarly the first order wave excitation forces and moments are obtained as

$$F_{Wi} = -\rho \iint_{S_w} (\tfrac{\partial\Phi_W}{\partial t} + gz)(n)_i ds \quad i = 1,2,3 \tag{2.6}$$

$$F_{Wi} = -\rho \iint_{S_w} (\tfrac{\partial\Phi_W}{\partial t} + gz)(r \times n)_i ds \quad i = 4,5,6 \tag{2.7}$$

where the wave excitation and force is separated into the incident and the diffracted or

$$\Phi_{Wi} = \Phi^I_{Wi} + \Phi^D_{Wi} \quad and \quad F_{Wi} = F^I_{Wi} + F^D_{Wi} \tag{2.8}$$

The hydrostatic restoring forces and moments are proportional to the displacement,

$$F_{hsi} = C_{ij} x_j$$

and the only non-zero linear coefficients are

$$\begin{aligned} C_{33} &= \rho g A_{WP} \\ C_{35} &= C_{53} = -\rho g \iint_{A_{WP}} x ds \\ C_{44} &= \rho g \nabla G M_T, \quad C_{55} = \rho g \nabla G M_L \end{aligned} \tag{2.9}$$

where A_{WP} is the water-plane area, ∇ is the displaced volume and GM_T and GM_L are the transverse and longitudinal metacentric heights respectively (see e.g. Biran, 2003).

2.2 Linear ship motions in regular waves

The Euler equations in (2.1) are coupled nonlinear equations not readily tractable even with the most advanced numerical schemes and often amount to exhaustible computer time and space. It also involves solving the three dimensional hydrodynamic problem of a body floating on the free surface. While the linear assumption is a limitation since it neglects viscous effects and characteristics of a real free surface, it has proven to be a tool that yields reasonable predictions for analysis at preliminary stages. One other advantage is the use of superposition principle which lends itself to admitting muti-harmonic forcing as is seen in the current thesis later with the consideration of pseudo random excitation. Thus apart from roll, linearization of the Euler equations provides a good approximation to the ship motion equations. Following a linearization scheme followed by Vugts (1970) the nonlinear inertial terms drop out from the Euler equations and the body rotation

rates and the Euler angle rates become an identity leading to linearized equations of the form:

$$\begin{aligned} X &= m[\dot{u} + z_G\dot{q}] \\ Y &= m[\dot{v} + x_G\dot{r} - z_G\dot{p}] \\ Z &= m[\dot{w} - x_G\dot{q}] \\ K &= I_{44}\dot{p} - I_{64}\dot{r} - mz_G\dot{v} \\ M &= I_{55}\dot{q} + m(z_G\dot{u} - x_G\dot{w}) \\ N &= I_{66}\dot{r} - I_{64}\dot{p} + mx_G\dot{v} \end{aligned} \tag{2.10}$$

Also to first order the rotation about a fixed or a moving system become identical. Now considering the excitation to be due to a single periodic wave with a surface elevation at the origin given by

$$\zeta(t) = \bar{\zeta}cos(\omega_e t + \epsilon) \tag{2.11}$$

where $\bar{\zeta}$ is the amplitude of the wave and ω_e is the frequency of encounter as observed by the ship, the vector of wave excitation force can be represented as

$$F_{Wi}(t) = F_{Wi0}\ cos(\omega_e t + \epsilon_{Wi0}) \quad i = 1, 2, ...6 \tag{2.12}$$

Depending on the wave heading angle, χ , the forward speed of the ship, V and the wave frequency, ω , the encounter frequency as observed in the body fixed system is defined by

$$\omega_e = \omega - \frac{\omega^2 V}{g} cos(\chi) \tag{2.13}$$

Radiation forces are proportional to the accelerations and velocities of ship motion. For the considered sinusoidal motion, the vector of radiation force components can be represented as

$$F_{ri} = -A_{ij}(\omega_e)\ddot{x}_j - B_{ij}(\omega_e)\dot{x}_j \quad i, j = 1, 2, ...6 \tag{2.14}$$

Using (2.14), (2.12) and (2.10), the frequency domain representation of the equations of motion become

$$[m_{ij} + A_{ij}(\omega_e)]\ddot{x}_j + B_{ij}(\omega_e)\dot{x}_j + C_{ij}x_j = F_{Wi}(t) \quad i,j = 1,2,...6 \tag{2.15}$$

where $A_{ij}(\omega_e)$ is the added mass coefficient matrix, $B_{ij}(\omega_e)$ is the damping coefficient matrix, and C_{ij} is the restoring force coefficient matrix. The only external forces are the Froude-Krylov force and the diffraction force given together by $F_{Wi}(t)$. It has to be noted that equation (2.15) would only be valid under the special case when the excitation force is single harmonic and only if the added mass and damping coefficients assume proper values at the excitation frequency, so the above equations can not really describe the ship motions in realistic seaway. Thus in the frequency domain representation of the equations of motion as in (2.15) above, the added mass and damping coefficients become functions of the excitation frequency. A more accurate representation of the time domain equations have constant added mass and the damping is expressed as a convolution integral. Furthermore, these equations (2.15) describe motion only in the steady state.

The true linear time domain equations of motion that describe the motion of ships in realistic seaway are given as follows (see e.g., Cummins, 1962)

$$[m_{ij} + A_{ij}(\infty)]\ddot{x}_j + \int_0^t K_{ij}(t-\tau)\ \dot{x}_j(\tau)\ d\tau + C_{ij}x_j = F_{Wi}(t) \quad i,j = 1,2,...6 \tag{2.16}$$

where $A_{ij}(\infty)$ is the added mass at infinite frequency, $K_{ij}(t-\tau)$, in the convolution integral, are the retardation functions of time which depend on the forward speed and the geometry of the vessel. They are the impulse response functions of the ship motion velocities and represent the memory effect of the radiated waves. The relation between $K_{ij}(t-\tau)$ and the frequency dependent damping coefficients $B_{ij}(\omega_e)$ is given by the following cosine transform (see, e.g., Ogilvie, 1964; Cummins, 1962)

$$K_{ij} = \frac{2}{\pi}\int_0^\infty B_{ij}(\omega_e)\ cos(\omega_e t)\ d\omega_e \tag{2.17}$$

2.3 Nonlinear large amplitude ship rolling in irregular waves

In order to understand the complicated dynamics observed in most capsizing studies to date it is essential not to ignore the important nonlinear effects of the ship motion equations. While this can be quite challenging or almost impossible to include them in the coupled six degrees of freedom, it is reasonable to isolate roll where the nonlinear viscous effects are most pronounced and attempt to analyze the dynamics in a more general treatment. This has been the focus of most nonlinear dynamical capsizing analyses who have used single frequency and single degree of freedom models (see, e.g., Falzarano 1990, Hsieh et al 1994, Jiang et al 1996), although mode coupling was considered in some cases (Zhang & Falzarano, 1994). A major part of the current thesis is to extend the significant work done by these previous groups while applying a new solution approach from the theory of nonlinear dynamics to the single degree of freedom in roll. Following (Falzarano, 1990), first order terms proportional to unit body motions are considered separately from the nonlinear damping and restoring forces. Linear hydrodynamic added mass $A_{ij}(\omega_e)\ddot{x}_j$, linear potential damping $B_{ij}(\omega_e)\dot{x}_j$ forces, wave exciting force F_{Wi} supplemented by the viscous roll damping and nonlinear hydrostatics $G(\dot{x}_4, x_4)$ are used, where x_4 represents the roll motion. Using these assumptions, the quasi-linear frequency domain equation of ship motion with nonlinear roll terms are given as follows

$$[m_{ij} + A_{ij}(\omega_e)]\ddot{x}_j + B_{ij}(\omega_e)\dot{x}_j + C_{ij}x_j + G(\dot{x}_4, x_4) = F_{Wi0}\ cos(\omega_e t + \epsilon_{Wi0}) \quad i, j = 1, 2, ...6 \quad (2.18)$$

For the fore-aft asymmetric ships, the above equation (2.18) implies a decoupling of sway, roll and yaw from surge, heave and pitch. This decoupling is preserved with the form of nonlinearity used to supplement the equations. Although sway is strongly coupled to roll, under certain conditions it is sometimes possible, by choosing an appropriate coordinate system (i.e. the roll center), to approximately decouple sway from roll (see e.g. Falzarano, 1990 or Roberts, 1986). Moreover, for a typical ship the coupling of yaw to roll and sway is less important than the coupling of sway to roll. Following Falzarano (1990), making all these assumptions, a frequency domain single degree of freedom roll equation of motion is obtained,

$$[I_{44} + A_{44}(\omega)]\ddot{\phi} + B_{44}(\omega)\dot{\phi} + B_{44q}\dot{\phi}|\dot{\phi}| + G(\phi) = F_{W40}\ cos(\omega_e t + \epsilon_{W40}) \quad (2.19)$$

where the encounter frequency is now same as the wave frequency for the roll equation considered in beam seas or from (2.13), $\omega_e = \omega(\chi = \frac{\pi}{2})$. In order to evaluate the nonlinear ship roll motion in the realistic sea way, we can consider the irregular wave excitation to be composed of a large finite number of periodic components with random relative phase angles, i.e.

$$F_{W4}(t) = \sum_{i=1}^{N} F_{W40i}\ cos(\omega_i t + \epsilon_{W40i}) \tag{2.20}$$

giving rise to an approximate representation of the roll equation of motion where constant values of the added mass and damping coefficients are assumed and are given by

$$[I_{44} + A_{44}(\omega)]\ddot{\phi} + B_{44}(\omega)\dot{\phi} + B_{44q}\dot{\phi}|\dot{\phi}| + G(\phi) = F_{W4}(t) = \sum_{i=1}^{N} F_{W40}\ cos(\omega_e t + \epsilon_{W40}) \tag{2.21}$$

Sea spectral models approximating a particular seaway intensity are often defined in terms of a single or multiple parameters such as significant wave height, peak period, peakedness or shape parameter etc.(Ochi, 1978). An example of a two parameter wave elevation spectrum in terms of the significant wave height, H_S , and the mean wave frequency, $\bar{\omega}$ called the Bretschneider spectrum is given below:

$$S^{+}(\omega) = 0.1107\ H_S^2 \frac{\bar{\omega}^4}{\omega^5}\ e^{(-0.4427(\frac{\bar{\omega}}{\omega})^4)} \tag{2.22}$$

In order to obtain the roll moment excitation spectra, the sea spectra is multiplied by the square of the roll moment excitation transfer function or the Response Amplitude Operator (RAO):

$$S_R^{+}(\omega) = S^{+}(\omega)|RAO(\omega)|^2 \tag{2.23}$$

where the roll transfer function (RAO) in general is obtained from the frequency dependent coupled linear response of the sway force and roll moment respectively or from standard sea-keeping programs which use the full six degree of freedom (6 DOF) linear equations of motions. They are

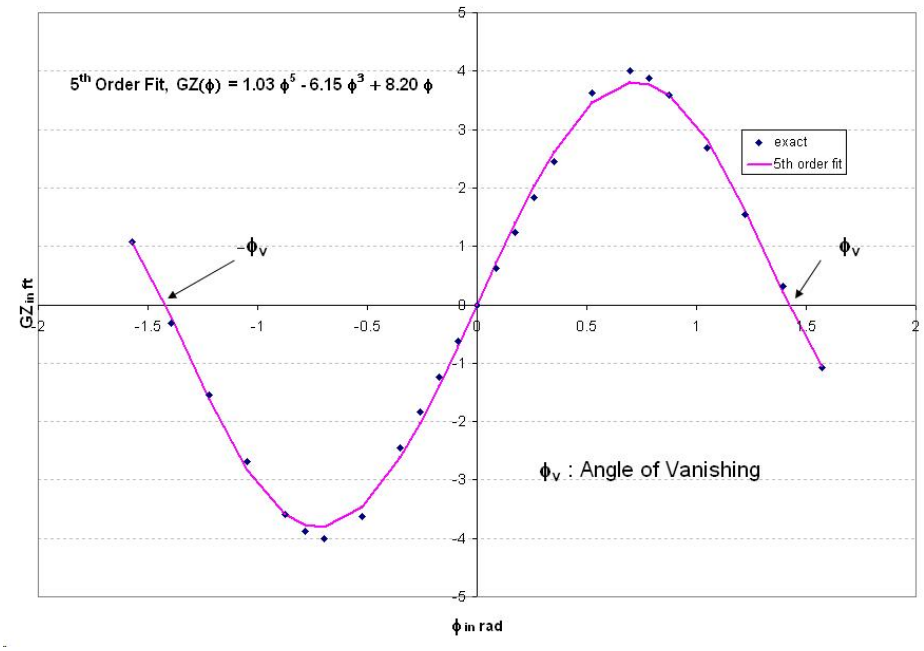

Fig. 2.2: Typical hydrostatic restoring moment characteristic, $GZ(\phi)$

a function of the geometry of the hull, loading condition and the frequency. It must be noted that the use of linear hydrodynamics in determining the roll excitation transfer function is one of the modeling limitations of the current method. The resulting roll moment excitation spectrum is then decomposed into harmonic components with random phase angles as given in equation (2.20) where

$$F_{W40i}(\omega_i) = \sqrt{2\ S_R^+(\omega_i)\Delta\omega} \tag{2.24}$$

One key feature of the equation(2.21) is the fact that it is not restricted to small motions as opposed to the linearized Euler equations. The restoring moment can in fact be computed theoretically from hydrostatics for specific hull forms. Figure 2.2 shows a sketch of a typical restoring moment characteristic showing the linear and a 5th order curve fit of the actual moment arm. Thus the linear hydrostatics (equation (2.9)) in roll are now replaced with a polynomial approximation of the nonlinear roll restoring moment (as a curve fit up to the 9th order) such as

$$G(\phi) = \Delta GZ(\phi) = \Delta(C_1 - C_3\phi^3 + C_5\phi^5 - C_7\phi^7 + C_9\phi^9) \tag{2.25}$$

which can admit values of roll till the angle of vanishing stability, ϕ_V. A characteristic of periodic

roll motion is that it is a resonant type of motion where large steady state amplitudes can result if the excitation frequency is close to the roll natural frequency (in cases where the nonlinearities in the hydrostatics are not pronounced) or close to the so-called throat region of the nonlinear resonance curve where multiple values in the roll amplitudes are possible (Falzarano, Vishnubhotla and Juckett, 2005). Also it is generally found that potential damping is very small in roll (Faltinsen, 1990) and corrections for total damping need to be made to account for the viscous effects. In equation (2.21), the linear potential damping $B_{44}(\omega)\dot{\phi}$ is supplemented with a nonlinear viscous damping term given by $B_{44q}\dot{\phi}|\dot{\phi}|$. This additional term includes the skin friction drag and effects due to flow separation, eddy making etc. Estimation of viscous hydrodynamic reaction force is not trivial and the current state of the art is to use

- Empirical methods as described in Himeno (1981);
- Experimental methods such as free decay tests of the model extrapolations or prototype and using energy methods to estimate the viscous damping coefficients (Faltinsen, 1990) or (Roberts, 1985);
- Theoretical and/or numerical techniques such as the (Reynolds Averaged Navier Stokes Solver) RANS (Korpus, Falzarano, 1996).

Thus we now have a more or less complete representation of large amplitude roll dynamics in its most general representation that includes the full nonlinear hydrostatics and the nonlinear viscous damping effects with the exception of the excitation force which is based on linear hydrodynamics. This is the focus of much of the work done in the current thesis and Chapter 3 deals with the solution methodology of the above equation using a perturbation technique of nonlinear dynamics, where, damping and forcing (which are usually an order of magnitude smaller in comparison to the restoring or the inertial forces in the roll equation), are considered as a perturbation to the unforced undamped system. However as discussed before a more accurate representation of the above equation in the time domain would be to use the convolution integral and represent a nonlinear time domain roll equation of motion as follows

$$[I_{44} + A_{44}(\infty)]\ddot{\phi} + \int_0^t K(t-\tau)\ \dot{\phi}(\tau)\ d\tau + B_{44q}\dot{\phi}|\dot{\phi}| + G(\phi) = \sum_{i=1}^{N} F_{4i}\ cos(\omega_i t + \epsilon_{4i}) \qquad (2.26)$$

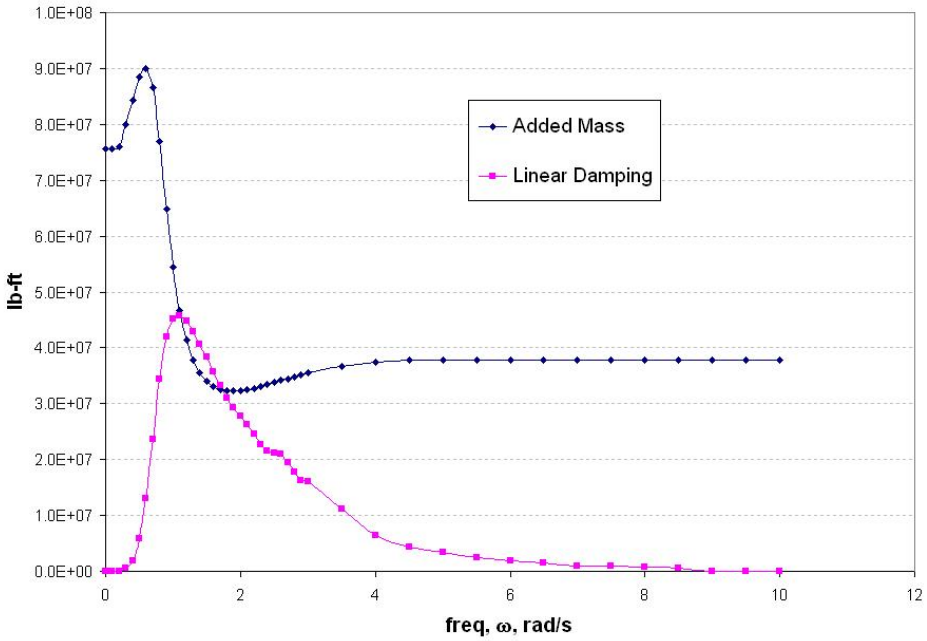

Fig. 2.3: Linear radiation forces, added mass and damping vs freq.

Sometimes equation (2.26) is also referred to as an integro-differential equation due to the presence of the convolution integral. Note that the added mass is a constant (at infinite frequency) in the above representation. Using equation (2.17) the impulse response function is obtained as an inverse Fourier cosine transform of the frequency dependent linear radiation damping. Figure 2.3 and Figure 2.4 show the linear radiation forces (added mass and damping) and the impulse response function for a traditional naval hull form DDG51.

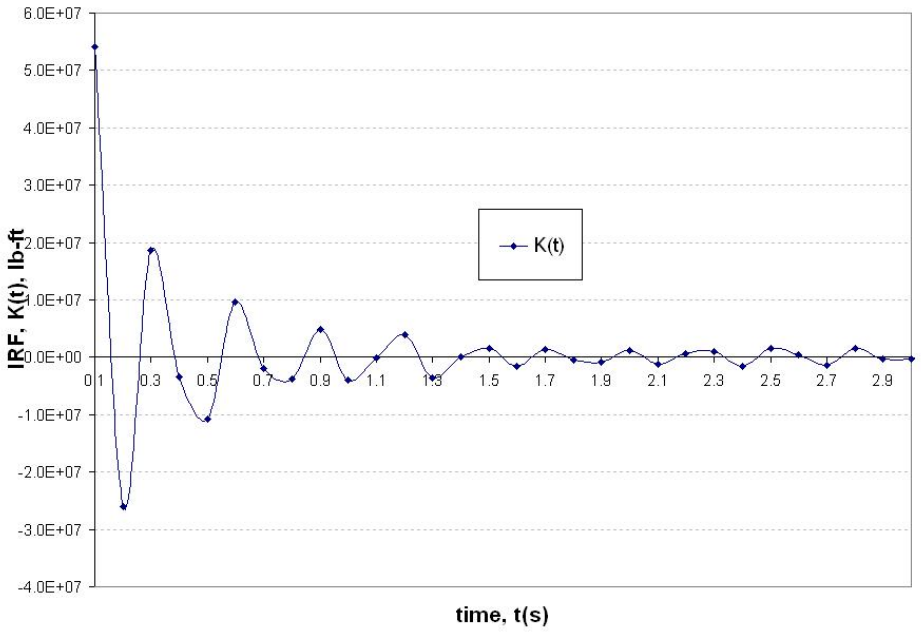

Fig. 2.4: Impulse response function, $K(t)$

3. APPLICATION OF VAKAKIS METHOD TO SHIP ROLLING

3.1 The problem of unbiased large amplitude rolling of a vessel in beam seas

The focus of this study is highly non-linear rolling motion possibly leading to capsizing. A closed form analytic solution following the dynamical perturbation method, is utilized to study the large amplitude roll motion of an unbiased ship at zero speed in beam random seas. In the non-linear dynamical systems theory, this procedure is an extension of Vakakis's approach to study the critical dynamics of the stable and unstable heteroclinic manifolds near the region of the ships angle of vanishing stability due to an irregular or pseudo random forcing function. Vakakis successfully applied this approach to explicitly express the stable and unstable homoclinic manifolds of an undamped periodically excited Duffing oscillator.

Although semi-submersibles generally have critical dynamics about a diagonal axis (Kota, Falzarano and Vakakis, 1998), in some cases for example the mobile offshore base single base units (MOB SBUs) due to the relatively large length to beam ratio, roll is still assumed to be critical. Roll is in general coupled to the other degrees of freedom, however under certain circumstances it is possible to approximately decouple roll from the other degrees of freedom and to consider it in isolation. This allows us to focus on the critical roll dynamics. The de-coupling is most valid for vessels which are approximately fore aft symmetric; this eliminates the yaw coupling. Moreover by choosing an appropriate roll-center coordinate system, the sway is approximately decoupled from the roll. For ships, it has been shown in previous studies that even if the yaw and sway coupling are included the results differ only in a quantitative sense. The yaw and sway act as passive coordinates and do not qualitatively affect the roll (Zhang and Falzarano, 1994).

The other issue is the modeling of the fluid forces acting on the hull. Generally speaking the fluid forces are subdivided into excitations and reactions. The wave exciting force is composed of a part due to incident waves and another due to the diffracted waves, F(t). These are strongly a

function of the wavelength / frequency. The reactive forces are composed of hydrostatic (restoring) and hydrodynamic reactions. The hydrostatic forces, $\Delta GZ(\phi)$, are most strongly non-linear and are calculated using a hydrostatics computer program. In order that the zeroth order solutions are expressed in terms of known analytic functions, the restoring moment curve needs to be approximated by a cubic polynomial. It should be noted here that it is not much more difficult to utilize a numerically generated zeroth order solution which is based upon an accurate higher order righting arm curve (Zhang and Falzarano, 1994).

The hydrodynamic part of the reactive force is that due to the so called radiated wave force. The radiated wave force is subdivided into added moment of inertia, $A_{44}(\omega)\ddot{\phi}$ and linear radiated wave damping $B_{44}(\omega)\dot{\phi}$. The two moment coefficients are strongly a function of frequency. However, since the damping is usually small, and for simplicity, constant values at a fixed frequency can be assumed resulting in a model approximation referred to as the constant coefficient model (CCM). In the next section, the solution procedure is outlined for the CCM approximation. The results obtained are then modified to include the frequency dependent added mass and damping under random forcing that encompasses a whole range of frequencies such as those due to a realistic seaway and is referred to as the convolution integral model (CIM). Generally, an empirically determined nonlinear viscous damping term, $B_{44q}(\omega)\dot{\phi}|\dot{\phi}|$, is included. However such results are only available for ship hulls. The resulting roll equation of motion using a CCM approximation where the linear added mass and damping are evaluated at a constant frequency ω is given by:

$$[I_{44} + A_{44}(\omega)]\ddot{\phi} + B_{44}(\omega)\dot{\phi} + B_{44q}\dot{\phi}|\dot{\phi}| + \Delta GZ(\phi) = F(t^*) = \sum_{i=o}^{N} F_{4i} \ \cos(\omega_i t^* + \epsilon_{4i}) \tag{3.1}$$

where I_{44} is the roll moment of inertia and Δ is the weight of the ship and $F(t^*)$ is the forcing due to the irregular sea obtained from the decomposition of the linear roll exciation spectra as discussed in the previous chapter. By defining a non-dimensionalized time t defined as shown below, equation (3.1) can be non-dimensionalized to

$$\ddot{x}(t) + \epsilon\delta\dot{x}(t) + \epsilon\delta_q\dot{x}(t)|\dot{x}(t)| + x(t) - kx^3(t) = \epsilon f(t) \tag{3.2}$$

where, $\epsilon\delta$ and $\epsilon\delta_q$ are the linear and non-linear damping coefficients respectively and k is the

strength of the cubic restoring non-linearity. If $GZ(\phi) = C_1\phi - C_3\phi^3$ and ω_n is the undamped roll natural frequency then the following non-dimensional terms in the above equation apply :

$$\begin{aligned} x = \phi, \quad t = t^*\omega_n, \quad \omega_n = \sqrt{\frac{\Delta C_1}{I_{44} + A_{44}(\omega)}}, \quad \epsilon\delta = \frac{B_{44}(\omega)}{(I_{44} + A_{44}(\omega))\omega_n}, \quad (\dot{}) = \frac{d}{dt} \\ \epsilon\delta_q = \frac{B_{44q}(\omega)}{(I_{44} + A_{44}(\omega))}, \quad \dot{x} = \dot{\phi}\ \omega_n^{-1}, \quad k = \frac{C_3}{C_1}, \quad \epsilon\gamma(t) = \frac{F(t^*)}{(I_{44} + A_{44}(\omega))\omega_n^2}, \quad \Omega = \frac{\omega}{\omega_n} \end{aligned} \tag{3.3}$$

It is important to note that the damping and the excitation are small (and scaled by a small quantity ϵ) and as noted by Falzarano (1990) this formulation allows us to consider the effects of damping and forcing on large vessel motions since the amplitude of motion is not restricted to be small. By defining $x(t) = u(t) = \phi(t)$ and $\dot{x}(t) = \dot{\phi}(t^*)\omega_n^{-1} = v(t)$, equation (3.2) can be expressed in the Cauchy (first order) standard form as :

$$\begin{aligned} \dot{u}(t) &= v(t) \\ \dot{v}(t) &= -u(t) + k\ u^3(t) + \epsilon\{-\delta v(t) - \delta_q v(t)|v(t)| + \gamma(t)\} \end{aligned} \tag{3.4}$$

For the unperturbed case, $\epsilon = 0$, the above equations represent the undamped rolling motion of an unbiased vessel in calm water. There are three fixed points for the system at $(u, v) = (0, 0)$ and $(\pm 1/k, 0)$ that represent a (stable) global centre at the origin and two unstable (hyperbolic) fixed points called saddles at the positive and negative angles of vanishing stability respectively. The associated phase plane consists of a symmetric pair of heteroclinic orbits connecting the saddle points given by:

$$u(t - t_0) = \pm\sqrt{\frac{1}{k}}\ \tanh(\frac{t - t_0}{\sqrt{2}}) \tag{3.5}$$

$$v(t - t_0) = \pm\sqrt{\frac{1}{2k}}\ \mathrm{sech}^2(\frac{t - t_0}{\sqrt{2}}) \tag{3.6}$$

The solutions to the above unperturbed equation with softening spring characteristics exhibit two greatly different types of motions depending upon the initial conditions with energy levels above

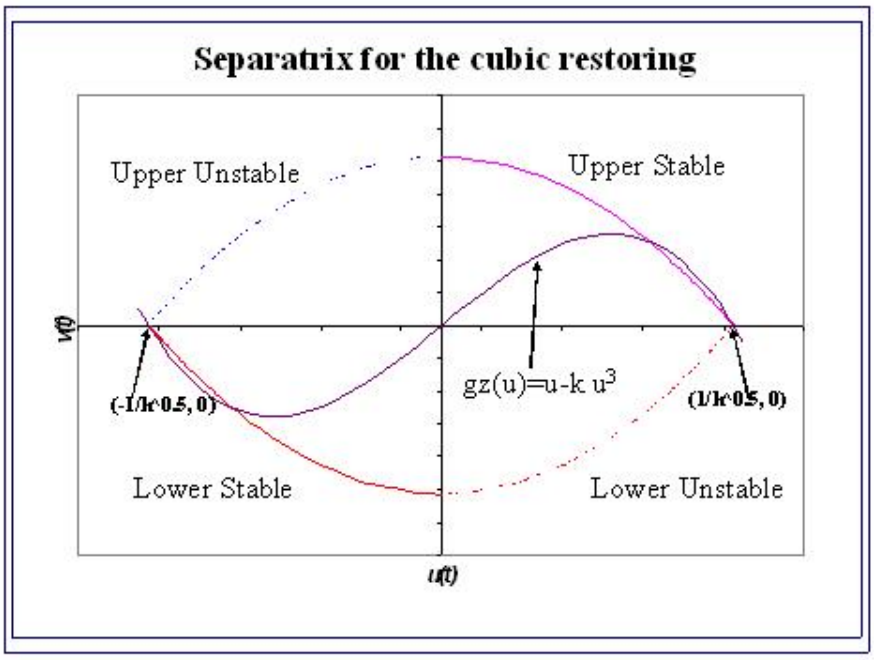

Fig. 3.1: Separatrix, manifolds for $\epsilon = 0$

or below the heteroclinic orbits. The curve or the boundary between these two types of motions is called in the terminology of nonlinear vibrations, the separatrix (also called the basin boundary), as it literally separates the two qualitatively different motions, see Figure 3.1. For initial conditions with small energy level (below the energy level along the separatrix) the first type of motion is an oscillatory motion which is bounded and well-behaved. Whereas initial conditions with energy levels above the energy level along the separatrix lead to unidirectional rotation which for a conventional vessel it represents an unbounded motion or capsize. These curves are also called the (upper and lower) saddle connections or *manifolds*. The saddles or the manifolds are connected as long as no damping and forcing are considered in the system. Once damping is added to the system, the saddle connection breaks into distinct stable (W^s) and unstable (W^u) manifolds (Figure 3.2). The stable manifolds are most important because they form the basin boundary between initial conditions which remain bounded and those that become unbounded. The key feature of this thesis is to be able to explicitly calculate these manifolds when damping and forcing are added to the system. The solution methodology is discussed in the following section.

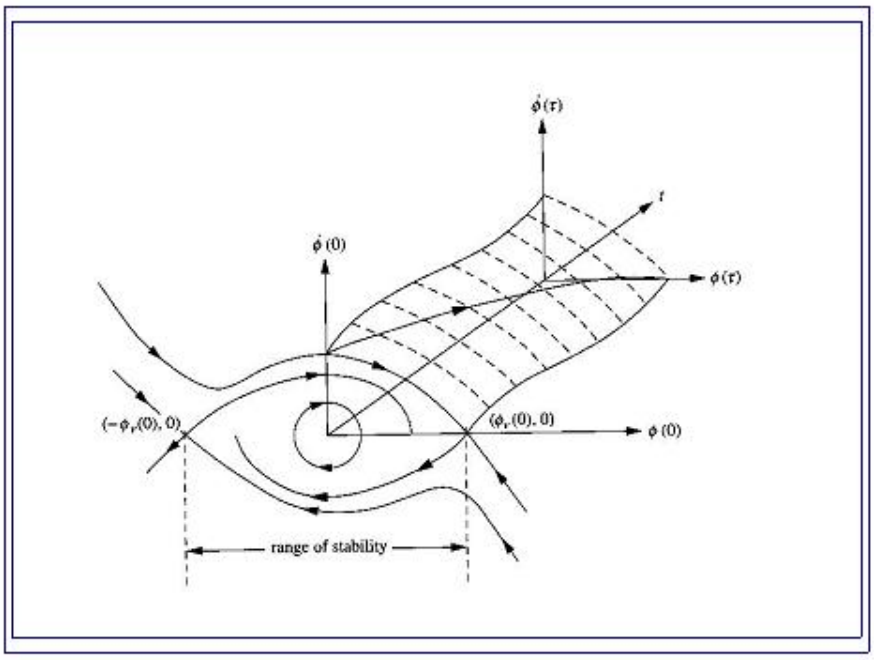

Fig. 3.2: Extended state space showing manifolds for, $\epsilon \neq 0$

3.2 Perturbational solution for small Damping, Forcing-Constant Coefficient Model

As already noted in the previous section when $\epsilon = 0$, equation (3.2) or system (3.4) is Hamiltonian or integrable and its phase plane contains the stable fixed point $(u, v) = p_0 = (0, 0)$ and two unstable ones, $p_{1,2} = (\pm 1/k, 0)$. The unperturbed phase plane possesses two heteroclinic orbits which result from the identification of the stable and unstable manifolds of the unstable fixed points. There are two basic perturbation results that follow (similar to the planar homoclinic orbits as discussed in Guckenheimer and Holmes, 1983):

1. For non-zero ϵ, sufficiently small and for a single periodic forcing, equation (3.2) possesses two unique hyperbolic periodic orbits,$\gamma_\epsilon(t) = p_{1,2} + O(\epsilon)$, of the saddle type which are ϵ -close to the unstable fixed points of the unperturbed problem. Correspondingly the Poincaré map, $P_\epsilon^{t_0}$ (sampling of the extended state space once per period of the forcing) has unique hyperbolic saddle points (Guckenheimer and Holmes, 1983).

2. The local stable and unstable manifolds of $\gamma_\epsilon(t)$ are C^r close ($r \geq 2$) to those of the unperturbed periodic orbit. Moreover orbits $x_{s,u}(t; t_0)$ lying on the stable and unstable manifolds

(denoted by subscripts s and u respectively) can be uniformly approximated in appropriate time intervals by series expressions of the form:

$$x_s(t;t_0;\epsilon) = x_{0,s}(t-t_0) + \sum_{n=1}^{\infty} \epsilon^n x_{ns}(t;t_0) \quad t \geq t_0 \tag{3.7}$$

$$x_u(t;t_0;\epsilon) = x_{0,u}(t-t_0) + \sum_{n=1}^{\infty} \epsilon^n x_{nu}(t;t_0) \quad t \leq t_0 \tag{3.8}$$

where t_0 denotes the initial time.

Substituting the above expressions in equation (3.2) and matching the coefficients of respective powers of ϵ, the equations governing the approximations of various orders are obtained. The zeroth order approximations correspond to motions on the heteroclinic orbits of the unforced autonomous system, and thus are invariant under any arbitrary time translations. By contrast the higher order approximations $x_{n,s,u}(t-t_0)$ are obtained by solving non-autonomous differential equations, and depend explicitly on the value of the initial time, t_0. The zeroth order approximation is computed, considering the unperturbed, unforced system:

$$\ddot{x}_{0,s,u} \; + x_{0,s,u} \; - k \; x_{0,s,u}^3 \; = 0 \Rightarrow \; x_{0,s} = x_{0,u} = \pm \frac{1}{\sqrt{k}} \; \tanh \frac{\eta}{\sqrt{2}} \tag{3.9}$$

where double dot denotes double differentiation with respect to η, and the notation $\eta = t - t_0$ is introduced. Similarly the equation governing the first order is given by

$$\ddot{x}_{1,s,u} \; + (1 - 3k \; x_{0,s,u}^2) x_{1,s,u} \; = \gamma(\eta + t_0) - \delta \; \dot{x}_{0,s,u} - \delta_q \; \dot{x}_{0,s,u} |\dot{x}_{0,s,u}| \; = \hat{f}(\eta) \tag{3.10}$$

Equation (3.10) is a linear differential equation with a parameter-dependent coefficient, and its general solution is obtained by using the method of variation of parameters (Ross, 1984)

$$\begin{aligned} x_{1,s,u}(\eta;t_0) = \big[\alpha_{1,s,u} \; - \int_0^{\eta} \hat{f}(\xi) x_{h1}^{(2)}(\xi) \; d\xi\big] x_{h1}^{(1)}(\eta) \\ + \; \big[\beta_{1,s,u} \; - \int_0^{\eta} \hat{f}(\xi) x_{h1}^{(1)}(\xi) \; d\xi\big] x_{h1}^{(2)}(\eta) \end{aligned} \tag{3.11}$$

where

$$x_{h1}^{(1)}(\eta) \; = \frac{1}{\sqrt{2k}} \mathrm{sech}^2 \frac{\eta}{\sqrt{2}} \; = \; \frac{dx_{0,s,u}}{d\eta} \tag{3.12}$$

$$x_{h1}^{(2)}(\eta) \ = 2^{1.5} k x_{h1}^{(1)}(\eta) \big[\frac{1}{4} \cosh^3 \frac{\eta}{\sqrt{2}} \ \sinh \frac{\eta}{\sqrt{2}} \ + \frac{3}{16} (\sinh \sqrt{2}\eta + \sqrt{2}\eta) \big] \tag{3.13}$$

are two linearly independent homogeneous solutions, and $\alpha_{1,s,u}$ and $\beta_{1,s,u}$ are constants evaluated so that $x_{1,s,u}(\eta; t_0)$ is bounded as $\eta \rightarrow \pm\infty$. In general for harmonic excitation it is seen that the first term in expression (3.11) is bounded while the second term is not. In fact the function $x_{h1}^{(2)}(\eta)$ diverges whereas the definite integral reaches a finite limit as $\eta \rightarrow \pm\infty$. Thus for bounded limits of $x_{1,s,u}(\eta; t_0)$ as $\eta \rightarrow \pm\infty$, it can be shown that the constants $\beta_{1,s,u}$ must be assigned the values $\beta_{1,s,u} \ = - \int_0^{\pm\infty} \hat{f}(\xi) \ x_{h1}^{(1)}(\xi) \ d\xi$ where the (+) and (-) signs on the upper limits of the integral refer to the subscripts s and u respectively. Thus the analytical solution to the orbits lying on the stable and unstable manifolds can be approximated up to the first order respectively by

$$x_s(\eta; t_0; \epsilon) = x_{0,s}(\eta) + \ \epsilon \ x_{1,s}(\eta; t_0) + O(\epsilon^2) \tag{3.14}$$

$$x_u(\eta; t_0; \epsilon) = x_{0,u}(\eta) + \ \epsilon \ x_{1,u}(\eta; t_0) + O(\epsilon^2) \tag{3.15}$$

It is finally noted that the constant $\alpha_{1,s,u}$ has an effect of time-shifting the zeroth order approximation by an amount equal to $\epsilon \ \alpha_{1,s,u}$ similar to the one predicted for the slowly forced Duffing system (Vakakis, 1994). Since the outlined perturbation analysis is carried out under the assumption of an initial time $t = t_0$ ($\eta = 0$), the constant $\alpha_{1,s,u}$ in (3.11) must be set equal to zero. The first order analytical solution to the orbits on the stable and unstable manifolds as derived can be extended to a pseudo random forcing function (for large N) where the function is expressed as a harmonic summation of N components with different amplitudes and random phase parameters (Vishnubhotla, Falzarano and Vakakis, 1998). For each individual component the boundedness of the analytical solution is assured as long as N is not infinite (Frey and Simiu, 1993, 1996) and hence for the total final solution to the first order.

3.3 Distance between the Manifolds and Equivalence to Melnikov Method

Consider an assumed time varying dynamical system of the form (Guckenheimer and Holmes, 1983) $\dot{x} = f(x) + \epsilon \ g(x,t) \quad x = q = (u,v) \in R^2$ where $f(x)$ is a known autonomous vector field and $g(x,t)$ is a time varying perturbation. Since we know the perturbed solutions to the first order we

use (3.14) and (3.15) to determine the separation of the manifolds as

$$d(t_0) = \epsilon \, \frac{f(x^0(0)) \ \wedge \ (q_{1,u}(t_0) - q_{1,s}(t_0))}{|f(x^0(0))|} \ + O(\epsilon^2) \tag{3.16}$$

This concept which was applied to homoclinic duffing oscillator by Vakakis is here utilized to estimate the separation of the manifolds for the heteroclinic ship/vessel problem. From equations (3.5) and (3.6) it follows that $f(x^0(0)) = (\frac{1}{\sqrt{2k}}, 0)$. Then if we let $VM(t_0) = f(x^0(0)) \ \wedge \ (q_{1,u}(t_0) - q_{1,s}(t_0))$, we get

$$VM(t_0) = f(x^0(0)) \ \wedge \ (q_{1,u}(t_0) - q_{1,s}(t_0)) = \frac{1}{\sqrt{2k}} \ (\dot{x}_{1,u}(t_0) - \dot{x}_{1,s}(t_0)) \tag{3.17}$$

where differentiating (3.11) with respect to time, it can be shown that

$$\dot{x}_{1,s,u}(t_0) = -\sqrt{2}\tanh(0) \ x_{1,s,u}(t_0) \ + \ 2^{-0.5}\big[\beta_{1,s,u} + \ \int_0^{\eta} \hat{f}(\xi) \ x_{h1}^{(1)}(\xi) \ d\xi\big] \ x_{h1}^{(2)}(0) \tag{3.18}$$

After some manipulation we have

$$VM(t_0) = \int_{-\infty}^{\infty} x_{h1}^{(1)}(\xi) \ \hat{f}(\xi) \ d\xi \equiv \int_{-\infty}^{\infty} f(x^0(t)) \ \wedge \ g(x^0(t), \ t + t_0) \ dt \tag{3.19}$$

It turns out that the left-hand-side of (3.19) is in fact identical to the one obtained using the Melnikovs method (the right-hand-side) where the zeros of the distance or the Melnikovs function correspond to transverse heteroclinic intersections of the manifolds as t_0 is varied. In the classical Melnikov method (to calculate the distance between the manifolds) the Melnikov integral is usually expressed in terms of the unperturbed $f(x)$ and the perturbed terms $g(x,t)$ of the governing equation evaluated along the unperturbed trajectories, $q_0(t) \equiv (x_0(t), \dot{x}_0(t))$. Therefore we never need to calculate the solutions to the perturbed equations. This results in a formula in terms of the system parameters and time. Simple zeros as t_0 is varied of the Melnikov function correspond to transverse heteroclinic intersections of the stable and the unstable manifolds. Specifically, from (3.14) and (3.15), the separation of the manifolds W^u and W^s can be defined on the section $\sum^{t_0}$ at the point $x^0(0)$ (Guckenheimer and Holmes, 1983) as $d(t_0) = x_\epsilon^u(t_0) - x_\epsilon^s(t_0) \ = \ \epsilon \, \frac{M(t_0)}{|f(x^0(0))|} \ + \ O(\epsilon^2)$ where $M(t_0)$ is defined as the Melnikov function and is determined by calculating an improper

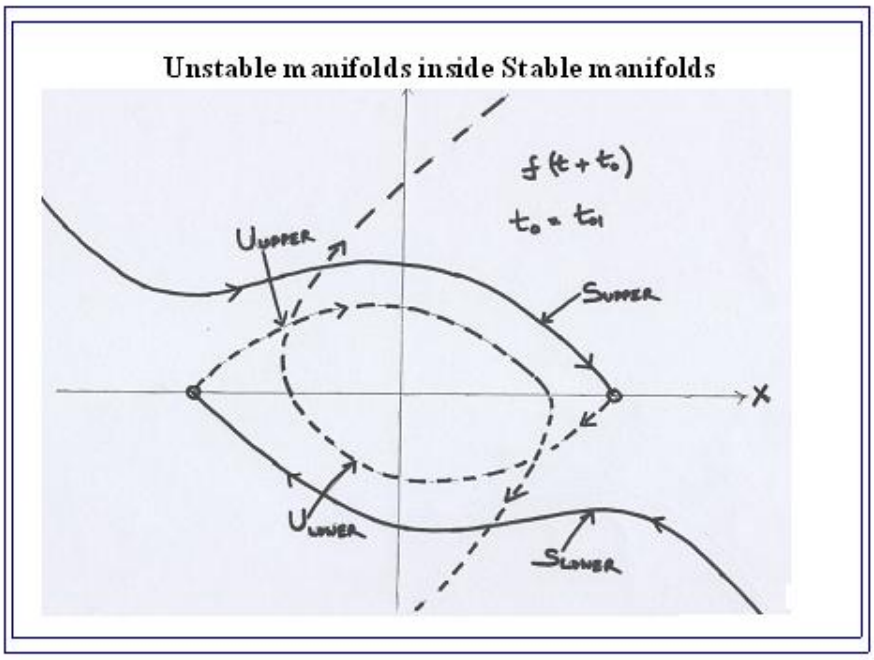

Fig. 3.3: Unstable manifolds inside stable for, $VM(t_0) < 0$

integral over all time ($-\infty < t < \infty$) also refrred to as the Melnikov integral,

$$M(t_0) = \int_{-\infty}^{\infty} f(q^0(t)) \ \wedge \ g(q^0(t),\ t + t_0)\ dt \tag{3.20}$$

which is same as (3.19) ($x \equiv q$).

The measure of the distance function $VM(t_0)$ developed herein or $M(t_0)$ (the classical Melnikov function which will be used from now on for the rest of the Chapter since they both have been shown to be equivalent) determine the relative orientation of the stable and unstable manifolds of the saddle points of the angles of vanishing stability. For small or zero forcing these functions are a negative constant for all time t_0. The unstable manifolds in such cases lie within the stable manifolds and the system is considered stable or safe, see Figure 3.3. Any initial condition starting within the stable manifolds will remain bounded or come to the upright equilibrium. However if the forcing is large enough that the Melnikov function is positive for all time the stable manifolds lie inside the unstable manifolds (upper or lower). Figure 3.4 shows the case when this happens for the upper manifolds (upper stable inside upper unstable). Figure 3.5 is an example when the function can be negative when the lower stable manifolds lie within the lower unstable. In either

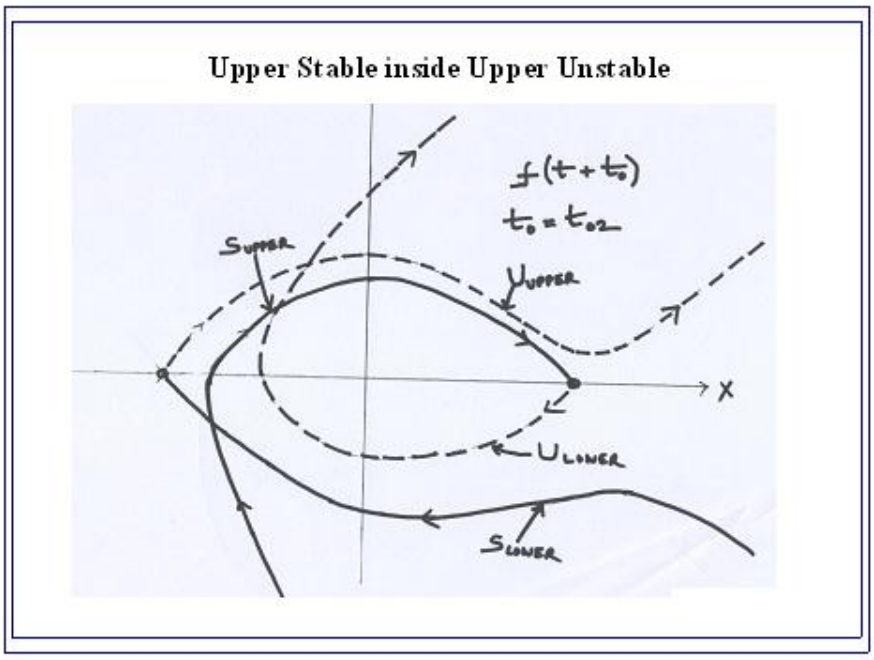

Fig. 3.4: Upper stable manifolds inside unstable for, $VM(t_0) > 0$

case this implies all the initial conditions starting near the basin boundary or the separatrix will lead to capsize. However there can be situations when manifolds cross one another as a function of time switching relative orientations. This is the situation referred to as chaos (Wiggins, 1990). The forcing is sufficiently large that the Melnikov function is positive for certain duration of the excitation and solutions between them will be transported out of the safe region. Chaotic transport theory shows that the area under the positive part of the Melnikov function is related to the rate at which solutions, quantified by phase space volumes, escape the safe basin. Although this has been utilized by Falzarano (1990) for harmonic excitaion and by Hsieh (1994) for random excitation a review of the results is presented in the next few sections to understand some of the results obtained using the chaotic transport theory and how they can be related to the likelihood of capsize for a given vessel under a given wave condition or a seaway.

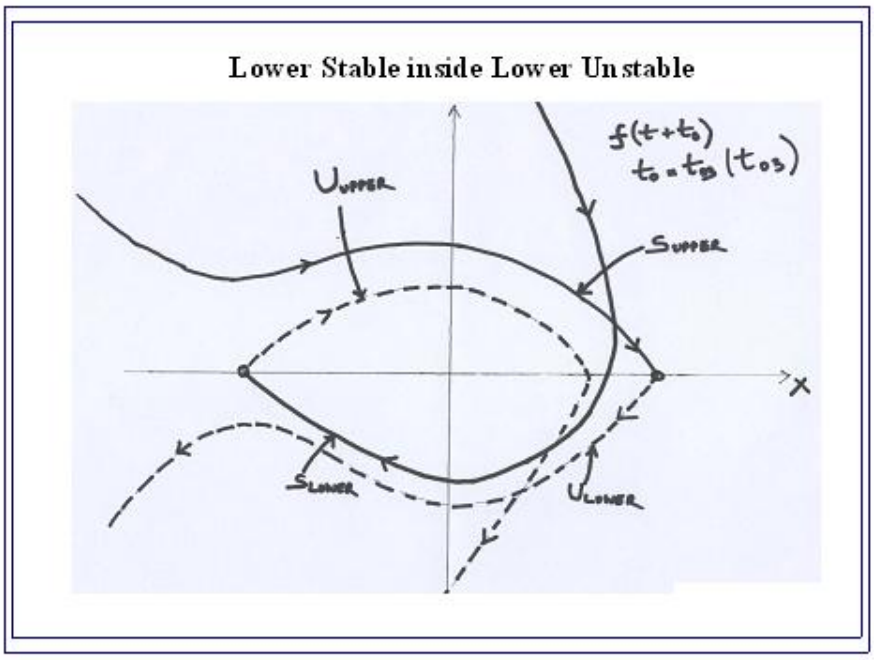

Fig. 3.5: Lower stable manifolds inside unstable for, $VM(t_0) > 0$

3.4 Melnikov function for single harmonic excitation

When the excitation is periodic or a harmonic function with a single frequency given by $\gamma(t) = \gamma\cos(\theta+\psi)$ or $\gamma(t) = \gamma\cos(\Omega t+\psi)$, equations (3.4) take the form

$$\begin{aligned}\dot{u}(t) &= v(t)\\ \dot{v}(t) &= -u(t) + k\ u^3(t) + \epsilon\{-\delta\ v(t) - \delta_q\ v(t)|v(t)| + \gamma\ \cos(\theta+\psi)\}\\ \dot{\theta} &= \Omega\end{aligned} \tag{3.21}$$

where ψ is a phase variable in the range $[0, 2\pi]$. The Melnikov function which provides a first order approximation of a measure for the separation of the manifolds for the above problem is given by

(Falzarano, 1990, Hsieh et. al, 1994)

$$
\begin{aligned}
M(t_0,\theta_0) &= \int_{-\infty}^{\infty} v_0(t)(-\delta\ v_0(t) - \delta_q\ v_0(t)\ |v_0(t)| + \gamma\ \cos(\Omega t + \Omega t_0 + \theta_0 + \psi))\ dt \\
&= \frac{2}{k}\gamma\ \pi\ \Omega\ \frac{\cos(\Omega t_0 + \theta_0 + \psi)}{\sinh\frac{\Omega\pi}{\sqrt{2}}} - \frac{2\sqrt{2}}{3k}\delta - \frac{8}{15}\ \frac{\delta_q}{k^{1.5}} \qquad (3.22) \\
&= \tilde{M}(t_0,\theta_0)\ -\ \overline{M}
\end{aligned}
$$

where $\overline{M}$ and $\tilde{M}(t_0,\theta_0)$ are, respectively, the constant and the oscillatory parts of the Melnikov function or

$$\overline{M} = \frac{2\sqrt{2}}{3k}\delta + \frac{8}{15}\ \frac{\delta_q}{k^{1.5}} \qquad (3.23)$$

$$\tilde{M}(t_0,\theta_0) = \frac{2}{k}\gamma\ \pi\ \Omega\ \frac{\cos(\Omega t_0 + \theta_0 + \psi)}{\sinh\frac{\Omega\pi}{\sqrt{2}}} \qquad (3.24)$$

Note that the function depends linearly on the amplitude of the excitation function and in a complicated fashion with the excitation frequency. Also for the unforced ($\gamma = 0$) system, the function is a negative constant, and this implies that hat the unstable manifolds of the saddle points near the angles of vanishing stability lie inside the stable manifolds. This means that the vessel with initial conditions located inside the unperturbed system (separatrix) will remain in the safe region. As the excitation amplitude is increased, the Melnikov function develops an oscillation about the negative mean value and there exists a certain critical excitation amplitude beyond which the function has nontangent or transversal zero crossings. This critical amplitude is given by

$$\gamma_{cr} = \frac{1}{\pi\Omega}\ (\frac{2\delta}{3\sqrt{k}}\ +\ \frac{4\sqrt{2}\ \delta_q}{15k})\ \sinh\frac{\pi\Omega}{\sqrt{2}} \qquad (3.25)$$

The existence of these zeroes implies that the phase space contains heteroclinic tangles, a scenario of global bifurcation resulting in complicated dynamics or chaos (Wiggins, 1990). One consequence of this situation is that the dynamics of the system started near the angle of vanishing stability are now essentially unpredictable and unexpected capsize may occur (Falzarano, 1990, 1992). Also the Melnikov function is now positive for certain phases of excitation and the area of the function which is positive is related to the phase space that is transported out of the safe region (Wiggins, 1990). The amount of phase space transported out in one period of excitation upto the first order

is given by

$$\nu = \epsilon \int_{t_{01}}^{t_{02}} M(t_0, \theta_0)\ dt_0\ + \emptyset(\epsilon^2) \tag{3.26}$$

where (t_{01}, t_{02}) denotes the time interval for which $M(t_0, \theta_0) > 0$. The average rate of phase space flux is then given by

$$\Phi = \epsilon\ \frac{\Omega}{2\pi}\ \int_{t_{01}}^{t_{02}} M(t_0, \theta_0)\ dt_0\ + \emptyset(\epsilon^2) \tag{3.27}$$

3.5 Melnikov function for multi harmonic excitation

The case in which the excitation is multi-harmonic,$f(t)$ can be represented as a summation of different frequencies and phases. Equation (3.21) will assume the form

$$\begin{aligned}
\dot{u}(t) &= v(t) \\
\dot{v}(t) &= -u(t) + k\ u^3(t) + \epsilon\{-\delta\ v(t) - \delta_q\ v(t)|v(t)| + \sum_{j=1}^{N} \gamma_j\ \cos(\theta_j + \psi_j)\} \\
\dot{\theta_j} &= \Omega_j \quad j = 1, 2, ...N.
\end{aligned} \tag{3.28}$$

Extending the result obtained before for a single frequency, the Melnikov function associated with the above equation is given by (Wiggins, 1992)

$$M(t_0, \bar{\theta}) = \tilde{M}(t_0, \bar{\theta}) - \overline{M} \tag{3.29}$$

$$\tilde{M}(t_0, \bar{\theta}) = \sum_{j=1}^{N} \frac{2}{k} \gamma_j\ \pi\ \Omega_j\ \frac{\cos(\Omega_j t_0 + \theta_{0j} + \psi_j)}{\sinh \frac{\Omega_j \pi}{\sqrt{2}}} \tag{3.30}$$

where $\tilde{M}(t_0, \bar{\theta})$ represents the oscillatory part of the Melnikov function and $\theta_0^j = (\theta_0^1, \theta_0^2, ...\theta_0^N)$ is a N-dimensional vector which represents the initial phase. Although in this case the details of the zero crossings and the phase space flux are more subtle the measure of the average rate of phase space flux is still obtained by using the generalized version of equation (3.27) and is given by

$$\Phi = \lim_{T\to\infty}\ \frac{\epsilon}{T}\ \int_{-T}^{T} M^+(\xi)\ d\xi \quad = \lim_{T\to\infty}\ \frac{\epsilon}{T}\ \int_{-T}^{T} (\tilde{M}(\xi) - \overline{M})^+\ d\xi \tag{3.31}$$

where the integrand represents the positive part of the Melnikov function.

3.6 Pseudo random or multi harmonic excitation with large N

Here we consider a limit where an input with a very large number of frequencies is used to model an irregular sea state (as discussed in the previous chapter). An arbitrary specified spectral density function $S_j^+(\Omega)$ is approximated by a finite sum of harmonic function (Rice, 1944) where the essential features of Rices work that a random process can be simulated by a series of cosine functions with weighted amplitudes, deterministic frequencies and random phase angles is utilized here again. Consider a random process with zero mean and one-sided power spectral function $S_j^+(\Omega)$ with insignificant magnitude outside the region defined by $\Omega_L \leq \Omega_j \leq \Omega_U$ where $(\Omega_L > 0)$ and $(\Omega_U < \infty)$ denote the lower and upper bounds of the frequency under consideration. The decomposition is achieved by truncating the continuous spectrum outside the range $[\Omega_L, \Omega_U]$ and dividing into N equally spaced frequency segments. The characteristic frequency associated with each individual frequency segment is defined by $\Omega_j = \Omega_L + (j - 0.5)\Delta_N$ for $1 \leq j \leq N$ where $\Delta_N = \frac{1}{N}(\Omega_U - \Omega_L)$ represents the width of each frequency segment. The magnitude associated with frequencyΩ_j is given by

$$\gamma_j = \sqrt{2A_j} = \sqrt{2S_j^+(\Omega_j)\Delta_N} \tag{3.32}$$

where A_j represents the area of the rectangular region formed by $S_j^+(\Omega)$ and Δ_N.

This yields sinusoidal oscillatory functions $\gamma_j \cos(\Omega_j t + \psi_j)$ for $j = 1, 2, .N$ in which ψ_j is a random phase angle uniformly distributed in $[0, 2\pi]$, resulting in a random function which is mean-ergodic and correlation-ergodic regardless of the number of frequencies (N) (Rice, 1944). As a consequence, the resultant Melnikov function is also mean-ergodic and correlation-ergodic (Hsieh, 1994). The mean and mean square of $\tilde{M}(t_0, \bar{\theta}_0)$ are given by

$$E[\tilde{M}(t_0, \bar{\theta}_0)] = E\left[\sum_{j=1}^{N} \sqrt{\frac{2}{k}} \frac{\gamma_j \Omega_j \pi}{\sinh(\frac{\Omega_j \pi}{\sqrt{2}})} \cos(\Omega_j t_0 + \theta_0^j + \psi_j)\right] = 0 \tag{3.33}$$

$$
\begin{aligned}
\sigma^2_{\tilde{M}} &= \frac{2}{k}\pi^2 \times \\
&E\Big[\sum_{i=1}^{N} \frac{\gamma_i\ \Omega_i}{\sinh(\frac{\Omega_i\pi}{\sqrt{2}})}\ \cos(\Omega_i t_0 + \theta_0^i + \psi_i)\Big] E\Big[\sum_{j=1}^{N} \frac{\gamma_j\ \Omega_j}{\sinh(\frac{\Omega_j\pi}{\sqrt{2}})}\ \cos(\Omega_j t_0 + \theta_0^j + \psi_j)\Big] \\
&= \frac{2}{k}\pi^2\ E\Big[\sum_{l=1}^{N} \frac{\gamma_l\ \Omega_l}{\sinh(\frac{\Omega_l\pi}{\sqrt{2}})}\ \cos(\Omega_l t_0 + \theta_0^l + \psi_l))^2\ +\ cross\ terms\Big] \\
&= \frac{2}{k}\pi^2\ E\Big[\sum_{l=1}^{N} \frac{1}{2}\ \big(\frac{\gamma_l\ \Omega_l}{\sinh(\frac{\Omega_l\pi}{\sqrt{2}})}\big)^2\ (1 + 2\cos(2\Omega_l t_0 + 2\theta_0^l + 2\psi_l))\Big] \\
&= \sum_{l=1}^{N} 2\pi S_f^+(\Omega_l)(\frac{\pi}{k})\ \big(\frac{\Omega_k}{\sinh(\frac{\Omega_l\pi}{\sqrt{2}})}\big)^2\ \Delta_N
\end{aligned}
\tag{3.34}
$$

where the cross terms have zero mean due to the independence of the phase angles ψ_i and ψ_j. By virtue of Central Limit Theorem (Lin, 1967), in the limit $N \to \infty$ $\tilde{M}(t_0, \bar{\theta}_0)$ is a Gaussian random variable with zero mean and standard deviation $\sigma_{\tilde{M}}$ and as $\Delta_N \to 0$

$$
\sigma^2_{\tilde{M}} = \int_0^{\infty} 2\pi S_f^+(\Omega)\big[\frac{\pi}{k}\big(\frac{\Omega}{\sinh\frac{\Omega\pi}{\sqrt{2}}}\big)^2\big]\ d\Omega \tag{3.35}
$$

Note that the expression $\frac{\pi}{k}\big(\frac{\Omega}{\sinh\frac{\Omega\pi}{\sqrt{2}}}\big)^2$ is the Fourier transform of the heteroclinic unperturbed solution $v_0(t)$. It must be pointed out however that the above limit $N \to \infty$ is taken only in a mathematically formal sense (Hsieh, 1994, Frey and Simiu, 1993) as a convenience to approximate sums of a large number of terms by a relatively simple integral. This is realized to ensure the mathematical conditions under which the Melnikov function is originally derived. In fact one cannot insure that the saddle point, which is the continuation of the angle of vanishing stability, remains a saddle-type invariant set in the limit $N \to \infty$.

The properties of the Menikov function can also be expounded using the standard definitions of auto-correlation function, spectral density function and their relationship via the *Wiener-Khintchine* relation. This is useful as shown by Hsieh et.al (1993) if the input excitation $f(t)$ were to be a continuous random process with zero mean and mean square spectral density $S_f(\Omega)$ and a corresponding one-sided mean square spectral density function $S_f^+(\Omega) = 2S_f(\Omega)$ defined over $\Omega > 0$. Invoking the definition of the Melnikov function with the assumption that $f(t)$ is now

random, we have

$$M(t_0) = \int_{-\infty}^{\infty} v_0(t)(-\delta\ v_0(t) - \delta_q\ v_0(t)\ |v_0(t)| + f(t+t_0))\ dt = \tilde{M}(t_0) - \overline{M} \tag{3.36}$$

where $\overline{M}$ is given by (3.23) and

$$\tilde{M}(t_0) = \int_{-\infty}^{\infty} v_0(t)\ f(t+t_0)\ dt \tag{3.37}$$

denotes the oscillatory part of the Melnikov function. Then the mean value of $\tilde{M}(t_0)$ is

$$E[\tilde{M}(t_0)] = E\big[\int_{-\infty}^{\infty} v_0(t)\ f(t+t_0)\ dt\big] = \int_{-\infty}^{\infty} v_0(t)\ E[f(t+t_0)]\ dt = 0 \tag{3.38}$$

since $E[f(t)] = 0$. Thus the oscillatory part of the Melnikov function is a random process with zero mean. This implies that $\overline{M}$ represents the mean value of $M(t_0)$. The mean square value of $\tilde{M}(t_0)$ is evaluated using the *Wiener-Khintchine* relation or

$$R_{\tilde{M}}(\tau) = \lim_{T\to\infty} \frac{1}{T} \int_{-\frac{T}{2}}^{\frac{T}{2}} \tilde{M}(t)\tilde{M}(t+\tau)\ d\tau = \int_{-\infty}^{\infty} S_{\tilde{M}}(\Omega) e^{j\Omega\tau}\ d\Omega \tag{3.39}$$

$$S_{\tilde{M}}(\Omega) = 2\pi \tilde{M}^*(\Omega)\ \overline{\tilde{M}^*(\Omega)} = \frac{1}{2\pi} \int_{-\infty}^{\infty} R_{\tilde{M}}(\tau) e^{-j\Omega\tau}\ d\tau \tag{3.40}$$

where $\tilde{M}^*(\Omega)$ is the Fourier transform of $\tilde{M}(t)$ given by $\tilde{M}^*(\Omega) = \frac{1}{2\pi}\int_{-\infty}^{\infty} \tilde{M}(\tau) e^{-j\Omega t}\ dt$ and an overline is used to denote complex conjugate. From the symmetry properties of $R(\tau)$ it follows that $S_g(\Omega) = S_g(-\Omega)$. Thus the mean square value of the oscillatory part of the Melnikov function can now be expressed in terms of its Fourier transform as

$$E[\tilde{M}^2(t_0)] = \lim_{T\to\infty} \frac{1}{T} \int_{-\frac{T}{2}}^{\frac{T}{2}} \tilde{M}^2(t_0)\ dt_0 = R_{\tilde{M}}(0) = \int_{-\infty}^{\infty} S_{\tilde{M}}(\Omega)\ d\Omega = \int_0^{\infty} S^+_{\tilde{M}}(\Omega)\ d\Omega \tag{3.41}$$

The Fourier transform of $\tilde{M}(t_0)$ is given by

$$\begin{aligned}
\tilde{M}^*(\Omega) &= \frac{1}{2\pi}\int_{-\infty}^{\infty}\Big(\int_{-\infty}^{\infty} v_0(t)f(t+t_0)\ dt\Big)\ e^{-j\Omega t_0}\ dt_0 \\
&= \frac{1}{2\pi}\int_{-\infty}^{\infty} v_0(t)\Big(\int_{-\infty}^{\infty} f(t+t_0)e^{-j\Omega t_0}\ dt_0\Big)\ dt \\
&= \frac{1}{2\pi}\int_{-\infty}^{\infty} v_0(t)\Big(\int_{-\infty}^{\infty} f(\xi)e^{-j\Omega \xi}\ dt_0\Big)\ dt\ e^{j\Omega t} \\
&= 2\pi\ f^*(\Omega)\ \overline{v_0^*(\Omega)}
\end{aligned} \tag{3.42}$$

Now considering the spectral density function of $\tilde{M}(t_0)$, $S_{\tilde{M}}(\Omega)$ and using (3.40) we get

$$\begin{aligned}
S_{\tilde{M}}(\Omega) &= 2\pi\ \tilde{M}^*(\Omega)\ \overline{\tilde{M}^*(\Omega)} \\
&= 2\pi\big(2\pi\ \overline{v_0^*(\Omega)}\ f^*(\Omega)\big)\ \big(2\pi\ v_0^*(\Omega)\ \overline{f^*(\Omega)}\big) \\
&= 2\pi\big(2\pi\ \overline{v_0^*(\Omega)}v_0^*(\Omega)\big)\ \big(2\pi\ f^*(\Omega)\overline{f^*(\Omega)}\big) \\
S_{\tilde{M}}(\Omega) &= 2\pi\ S_{v_0}(\Omega)\ S_f(\Omega)
\end{aligned} \tag{3.43}$$

The one-sided spectral density of $\tilde{M}(t_0)$ is then given by (3.43) which is

$$S^+_{\tilde{M}}(\Omega) = 2\ S_{\tilde{M}}(\Omega) = 2\ \big(2\pi\ S_{v_0}(\Omega)\ S_f(\Omega)\big) = 2\pi\ S_{v_0}(\Omega)\big(2\ S_f(\Omega)\big) = 2\pi S_{v_0}(\Omega)\ S^+_f(\Omega) \tag{3.44}$$

and is defined over $\Omega > 0$. The mean square value of $\tilde{M}(t_0)$ is then given by

$$E[\tilde{M}^2(t_0)] = \int_{-\infty}^{\infty} S_{\tilde{M}}(\Omega)\ d\Omega = \int_0^{\infty} S^+_{\tilde{M}}(\Omega)\ d\Omega = \int_0^{\infty} 2\pi\ S_{v_0}(\Omega)\ S^+_f(\Omega)\ d\Omega \tag{3.45}$$

3.7 Phase space flux and critical criterion for pseudo random excitation

An expression for the rate of phase space flux as developed by Hsieh (1994) using the Melnikov function as developed for pseudo random excitation is re-worked here. The result states that upto the first order the area under the positive part of the Melnikov function represents the area being transported out of the pseudo-separatrix of the heteroclinic orbit. It is a generalized extension of the lobe dynamics (Wiggins, 1990) well developed for the periodic excitation and successfully utilized by previous studies (Falzarano, 1990).

Based on the previous analysis, we now know that the Melnikov function $M(t_0)$ is a random

process with Gaussian distribution. Furthermore the resultant Melnikov function is stationary and ergodic (Hsieh, 1994). Hence the values of the mean $\overline{M}$ and the variance $\sigma^2_{\tilde{M}} = E[\tilde{M}^2(t_0)]$ completely characterize $M(t_0)$. Also we know from statistical theory that if a random process is stationary and ergodic the temporal average is equal to the ensemble average. It is precisely this characteristic that makes the rate of phase space flux, which in expressed in terms of the Melnikov function, amenable for pseudo random excitation. Hence using equation (3.31) we have

$$\Phi = \lim_{T\to\infty} \frac{\epsilon}{2T} \int_{-T}^{T} M^+(\xi)\ d\xi = \epsilon\ E[M^+(\xi)] = \epsilon\ E[\tilde{M}(\xi) - \overline{M})^+] \tag{3.46}$$

Evaluating the integral further, we get

$$\begin{aligned}
\Phi(\sigma, \overline{M}) &= \epsilon\ E[(\tilde{M}(\xi) - \overline{M})^+] = \epsilon \int_{\overline{M}}^{\infty} (z - \overline{M})\ p(z)\ dz \\
&= \epsilon \int_{\overline{M}}^{\infty} (z - \overline{M}) \big(\frac{1}{\sqrt{2\pi}\ \sigma}\big)\ e^{\big(-\frac{z^2}{2\sigma^2}\big)}\ dz \\
&= \epsilon\ \sigma \int_{\frac{\tilde{M}}{\sigma}}^{\infty} \big(z - \frac{\tilde{M}}{\sigma}\big)\ \big(\frac{1}{\sqrt{2\pi}}\big)\ e^{\big(-\frac{x^2}{2}\big)}\ dx \\
&= \epsilon\ \big(\sigma\ p_n(\frac{\overline{M}}{\sigma}) + \overline{M}\ P_n(\frac{\overline{M}}{\sigma}) - \overline{M}\big)
\end{aligned} \tag{3.47}$$

where $p(z)$ denotes the probability density function of $M(t_0)$, and

$$p_n(z) = \frac{1}{\sqrt{2\pi}}\ e^{\big(-\frac{z^2}{2}\big)}\ dz \tag{3.48}$$

$$P_n(z) = \int_{-\infty}^{\infty} p_n(\xi)\ d\xi \tag{3.49}$$

represent, respectively, the probability density and distribution functions of the standard Gaussian random variable. The simple steps needed to calculate the rate of phase space flux as given by equation (3.47) can be summarized again as follows (Hsieh, 1994):

- Determine the system parameters (specifically $k, \epsilon, \delta, \delta_q$) which determine $\overline{M}$;
- Evaluate the Fourier transform of the unperturbed heteroclinic solution $v_0(t)$ and from the one-sided spectral density function $S_f^+(\Omega)$ that describes any given sea-state, one can evaluate the mean square value of the random Melnikov function;

- Finally using equation (3.47) compute the rate of phase space flux using the definitions for the probability density function of a standard Gaussian random variable;

The focus of attention is then to investigate how the rate of the phase space flux relates to the onset of capsize. Following Hsieh (1994) the critical wave height at which substantial phase-space flux begins to occur, suggesting an increased risk of operating the vessel, is given by

$$H_s^* = \frac{\sqrt{2\pi}\ \overline{M}}{2\sigma^1} \tag{3.50}$$

where σ^1 refers to the RMS (root-mean-square) value of $\tilde{M}(t_0)$ for unit significant wave height (see Hsieh (1994) for discussion).

3.8 Problem Formulation for Convolution Integral Model

The coefficients in the previous sections, $A_{44}(\omega)$ and $B_{44}(\omega)$, are frequency dependent because of the presence of free surface. If the excitation is single harmonic, then the coefficients take on the value of the excitation frequency. For the pseudo random excitation considered in the current work, the coefficients previously were taken at the characteristic wave frequency $\bar{\omega}$ or ω_z of the input wave spectrum spectrum $S_\zeta^+(\omega)$ leading to the formulation of the roll equation (3.1) called the constant coefficient model (CCM). This has been shown to be a reasonable approximation for a narrow-banded excitation (Holappa and Falzarano, 1999). For excitations with wide band spectra roll natural frequency, ω_n may be better.

However if the forcing is not single harmonic, the frequency dependence of the coefficients (Ogilvie, 1964) must be accounted for in the time domain roll equation of motion. This leads to a more accurate representation of the roll equation given by:

$$[I_{44}+A_{44}(\infty)]\ddot{\phi}+\int_0^t K(t-\tau)\ \dot{\phi}(\tau)\ d\tau+B_{44q}\dot{\phi}|\dot{\phi}|+\Delta GZ(\phi) = F(t^*) = \sum_{i=o}^{N} F_{4i}\ \cos(\omega_i t^*+\epsilon_{4i}) \tag{3.51}$$

The instantaneous hydrodynamic moment due to $\phi(t)$ is the hydrostatic roll restoring given by $\Delta GZ(\phi) = \Delta(C_1\phi - C_3\phi^3)$ for a cubic approximation of the hydrostatic moment curve. Although a cubic approximation is used here for simplicity it must be noted that the method developed in the current work can handle any form of angle dependent hydrostatic moment and is valid for large

angles of roll. The hydrodynamic reaction moments due to $\dot{\phi}(t)$ and $\ddot{\phi}(t)$ are the linear radiation moment forces. $A_{44}(\infty)$ is the added mass coefficient evaluated at infinite frequency and in fact is a constant that depends only the ship geometry. $[I_{44} + A_{44}(\infty)]\ddot{\phi}$ represents the total linear hydrodynamic roll moment reaction due to the instantaneous $\ddot{\phi}(t)$.

$K(t)$ represents the hydrodynamic roll moment due to a unit impulse roll velocity where the response lasts longer than the duration of the impulse (Cummins, 1962). The integral of $K(t-\tau)\ \dot{\phi}(\tau)$ represents the cumulative sum of the responses due to a history of roll velocity impulses, each response calculated with an appropriate time lag from the instant of the impulse. Denoting this formulation as the convolution integral model, CIM (due to the convolution integral in the differential roll euqtion of motion) we note that unlike the hydrodynamic reaction moments that change instantaneously with $\phi(t)$ and $\ddot{\phi}(t)$ the influence from $\dot{\phi}(t)$ is cumulative and will be present for sometime before it dies out. The relation between $K(t)$ and the frequency dependent linear coefficients, $B_{44}(\omega)$ and the evaluation of $K(t)$ from a regular ship motion analysis was discussed in Chapter 2. The quadratic damping coefiicient $B_{44q}(\omega)$ is found by model tests and is assumed to be a constant in the current work.

We can also re-write equation (3.51) by expanding the limits of integration in the convolution integral to $(-\infty, \infty)$ since it is understood that $\dot{\phi}(t) = 0, t < 0$ and $K(t) = 0, t < 0$ from the principle of *causality*. And since $\int_{-\infty}^{\infty} K(t-\tau)\ \dot{\phi}(\tau)\ d\tau\ \equiv\ \int_{-\infty}^{\infty} K(\tau)\ \dot{\phi}(t-\tau)\ d\tau$ we have

$$[I_{44}+A_{44}(\infty)]\ddot{\phi}+\int_{-\infty}^{\infty} K(\tau)\ \dot{\phi}(t-\tau)\ d\tau+B_{44q}\dot{\phi}|\dot{\phi}|+\Delta(C_1\phi-C_3\phi^3)=\sum_{i=o}^{N} F_{4i}\ \cos(\omega_i t^*+\epsilon_{4i}) \quad (3.52)$$

Non-dimensionalizing equation (3.52) as we did for the CCM we have

$$\ddot{x}(t)+\epsilon\int_{-\infty}^{\infty}\kappa(t)\ \dot{x}(t-\tau)\ d\tau+\epsilon\delta_q\dot{x}(t)|\dot{x}(t)|+x(t)-kx^3(t)=\epsilon f(t) \quad (3.53)$$

$$\begin{gathered} x=\phi,\quad t=t^*\omega_n,\quad \omega_n=\sqrt{\frac{\Delta C_1}{I_{44}+A_{44}(\infty)}},\quad \epsilon\kappa(t)=\frac{K(t)}{I_{44}+A_{44}(\infty)} \\ \epsilon\delta_q=\frac{B_{44q}(\omega)}{I_{44}+A_{44}(\infty)},\quad k=\frac{C_3}{C_1},\quad \epsilon\gamma(t)=\frac{F(t^*)}{(I_{44}+A_{44}(\infty))\omega_n^2},\quad \Omega=\frac{\omega}{\omega_n} \end{gathered} \quad (3.54)$$

Similar to the CCM solution approach, the zeroth order solutions for CIM, in the application of the dynamical perturbation method, are still given by equations (3.5) and (3.6) respectively. However the right hand side of the first-order equation (3.10) must be re-addressed and is not as straight forward as before.

$$\begin{aligned}\hat{f}(\eta) &= \gamma(\sqrt{2}\eta + t_0) - \delta \int_{-\infty}^{\infty} \kappa(\tau)\ \dot{x}_{0,s,u} d\tau - \delta_q\ \dot{x}_{0,s,u}|\dot{x}_{0,s,u}| \\ \hat{f}(\eta) &= \gamma(\sqrt{2}\eta + t_0) - \delta \int_{-\infty}^{\infty} \kappa(\tau)\ v_0(\eta - \tau) d\tau - \delta_q\ v_0(\eta)|v_0(\eta)|\end{aligned} \tag{3.55}$$

As can be seen that the function $\hat{f}$ is modified from equation (3.10) due to the presence of the convolution of $\kappa(t)$ and $v_0(t)$. This is determined numerically by a combination of fast Fourier transform and an inverse fast Fourier transform technique. After this the solution methodology of the perturbed manifolds is similar to the procedure followed for the CCM formulation discussed previously.

The Melnikov function for the CIM formulation is also not as straight forward since the integral term in the perturbation does not depend simply on the instantaneous values of the system states and time, but on the history of the roll velocity. Jiang (1996) used a standard approach that approximates the memory effects by the output of a finite-dimensional linear dynamical system to modify the Melnikov theory. The outcome of the results show that one can procedurally treat the integral perturbation term in the usual manner that has been developed for perturbations of planar systems (Jiang, 1996). Melnikov function in this case is given by

$$M(t_0) = \int_{-\infty}^{\infty} v_0(t)(-\int_{-\infty}^{\infty} \kappa(\tau)\ \ v_0(t-\tau)\ d\tau\ \ - \delta_q\ v_0(t)\ |v_0(t)| + f(t+t_0))\ dt = \tilde{M}(t_0) - \overline{M} \tag{3.56}$$

where the oscillatory part $\tilde{M}(t_0)$ is given as before by equation (3.37) and the constant part is modified as

$$\overline{M} = \int_{-\infty}^{\infty} v_0(t)\ \Big(\int_{-\infty}^{\infty} \kappa(\tau)\ \ v_0(t-\tau)\ d\tau\ \Big)\ dt\ + \frac{8}{15}\ \frac{\delta_q}{k^{1.5}} \tag{3.57}$$

Evaluation of the modified constant part of the Melnikov function is handled similar to the perturbed solution approach by using the fast Fourier and inverse fast Fourier transforms respectively.

4. RESULTS AND OBSERVATIONS

4.1 Comparison with Numerical Integration, periodic forcing

The dynamical perturbation solution approach for calculating the stable and the unstable manifolds is compared with the solutions obtained from numerical nonlinear differential equation solver program (Parker & Chua, 1989). A twice capsized small fishing boat called *Patti*-B is used for the comparison of results. Excitation resulting from a periodic forcing from a wave amplitude of 0.75 m (or 5 ft wave height) at 0.7 rad/s is chosen. A cubic fit for the nonlinear restoring moment is utilized while matching the units roll angle of vanishing stability, ϕ_v at 0.5647 rad. Table 4.1 below gives the details of the vessel particulars.

Any projected phase plane in 2-D of the stable and the unstable solution orbits lying in a three dimensional space at integer multiples of forcing period is referred to as a Poincaré map and is schematically shown in Figure 3.2 of Chapter 3. A family of such orbits make up the respective stable and unstable manifolds. Figure 4.1 however shows a two dimensional projection of the stable and unstable manifolds from the perturbation solution approach. Alternatively Figure 4.2 shows the Poincaré map (which is essentially a stroboscopic sampling) of the manifolds at one period of the forcing function or at 8.97 s respectively. Also seen in both the figures are the periodic solution orbits whose fixed points given by (ϕ_y, 0) (0.5634 rad., 0) and (-ϕ_y, 0) (-0.5660 rad., 0) respectively which lie close to the corresponding angles of vanishing stability, ($\pm\phi_v$, 0) = (0.5647 rad., 0). Figure 4.3 shows the comparison between the analytical (perturbation solution) and numerical approaches for the upper stable and the lower unstable manifolds of *Patti*-B.

The results compare (see Figure 4.3) quite well at least in the intervals of time when the perturbation method is applicable i.e for $t > t_0$ for the stable manifolds and $t < t_0$ for the unstable manifolds respectively for the current example). Another interesting observation from the perturbation (analytical) results is the diverging behavior of the unstable manifolds as opposed to

Parameter	Units	Dimensional Value
Length of the boat, L	m	22.90
Displacement, Δ	N	2370000.00
Linear restoring arm, C_1	m	0.214
Nonlinear restoring arm, C_3	m	0.671
Wave amplitude, ζ	m	0.75
Forcing frequency, ω	rad/s	0.70
Linear natural frequency, ω_n	rad/s	0.593
Hydrodynamic mass, $(I_{44} + A_{44}(\omega))$	kg-m^2	1470000.00
Linear damping, $B_{44}(\omega)$	kg-m^2-s^{-1}	5480.00
Nonlinear damping, B_{44q}	kg-m^2	98800.00
Total wave force, $F_{44}(\omega)$	N-m^{-1}	3010.00

Tab. 4.1: Parameters for fishing boat *Patti*-B

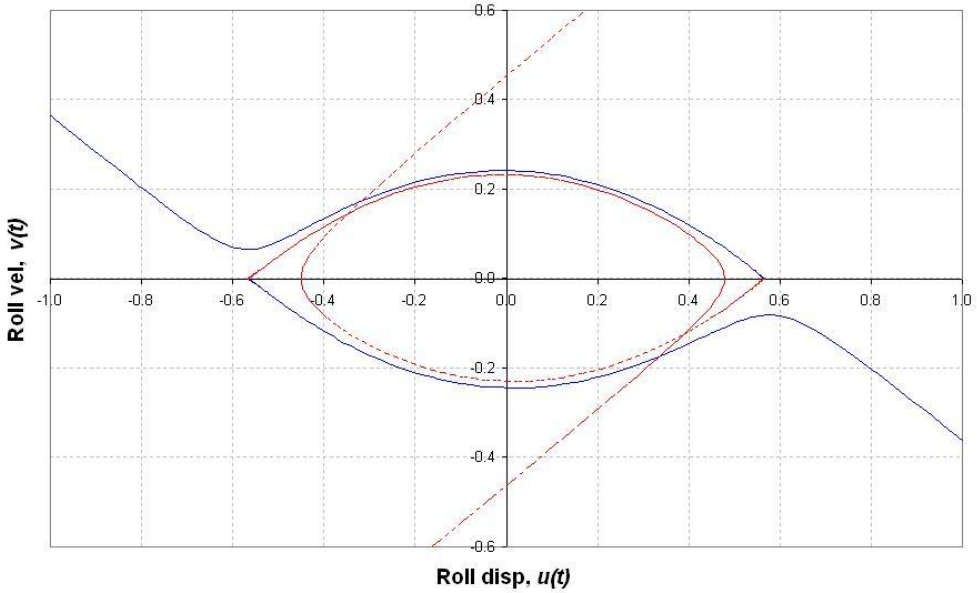

Fig. 4.1: Patti-B stable (solid) and unstable (dotted) manifolds - perturbation

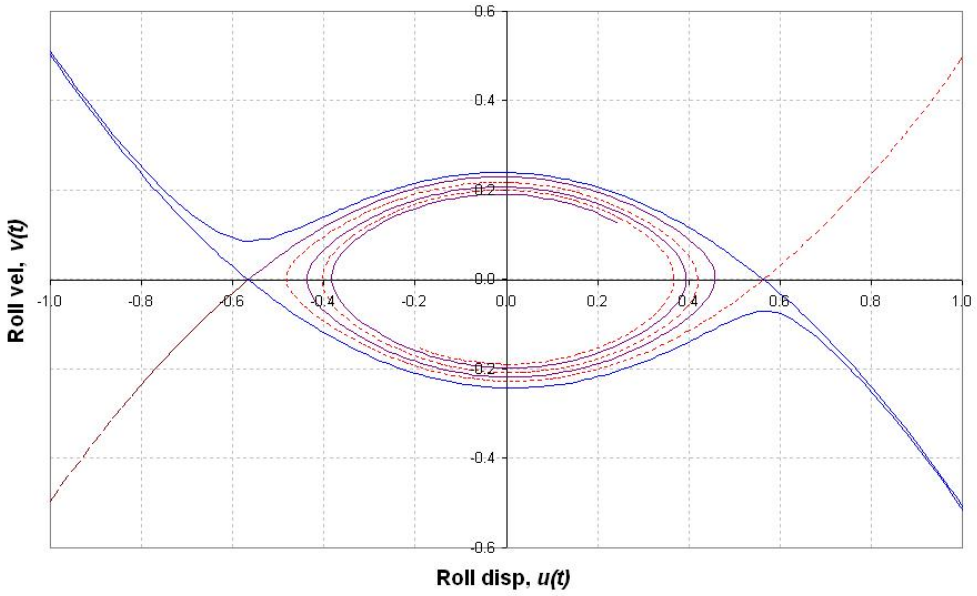

Fig. 4.2: Patti-B stable (solid) and unstable (dotted) manifolds - numerical

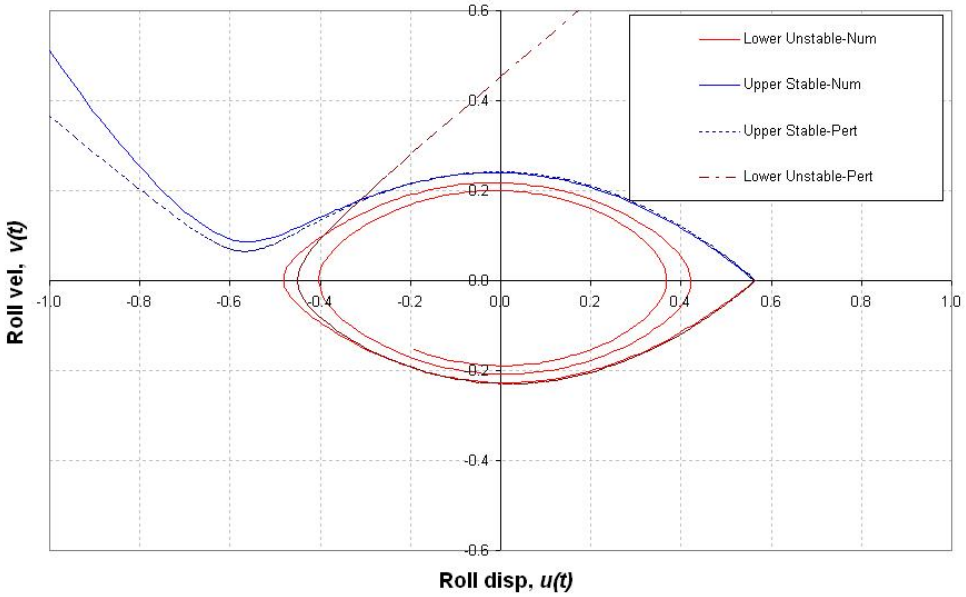

Fig. 4.3: Comparison of upper stable and lower unstable manifolds (perturbation vs. numerical)

Parameter	Units	Dimensional Value
Length of the vessel, L	ft	466.00
Displacement, Δ	lb	18900000.00
Linear restoring arm, C_1	ft	6.570
Nonlinear restoring arm, C_3	ft	3.120
Wave amplitude, ζ	ft	5.70
Forcing frequency, ω	rad/s	0.90
Linear natural frequency, ω_n	rad/s	0.572
Hydrodynamic mass, $(I_{44} + A_{44}(\omega))$	slug-ft^2	380000000.00
Linear damping, $B_{44}(\omega)$	slug-ft^2-s^{-1}	1810000.00
Nonlinear damping, B_{44q}	slug-ft^2	18400000.00
Total wave force, $F_{44}(\omega)$	lb-ft^{-1}	4125000.00

Tab. 4.2: Parameters for the traditional naval hull DDG-51

those from the numerical method where they lie (and expectedly so) within the boundary of the stable manifold. This behavior is also explained based on the intervals of validity of the perturbation method and this is one of the limitations of using the analytic solution beyond their domains of definition. However it must be pointed out that in the domain of interest the solutions match closely (numerical versus the perturbation (analytical) solution).

4.2 Comparison of current method to (classical) Melnikov approach (periodic forcing)

While the previous example was for a small fishing vessel with moderate forcing, we now consider a traditional navy hull form forced under a more severe condition where critical roll dynamics leading to capsize could occur. The roll natural period of these hull forms are in the range of 9 to 15 seconds which is also where most of the seaway intensity for wave forcing is generally distributed making the stability of these units very sensitive to dynamic effects. Table 4.2 gives the details of the vessel particulars where a cubic curve fit is again used to approximate the nonlinear restoring moment and the roll angles of vanishing stability at $\phi_v = 1.451$ rad. Periodic excitation from a wave amplitude of 5.7 ft (or 11.4 ft wave height) at 0.9 rad/s is chosen.

The hydrodynamic wave force and the linear radiation forces (added mass and potential

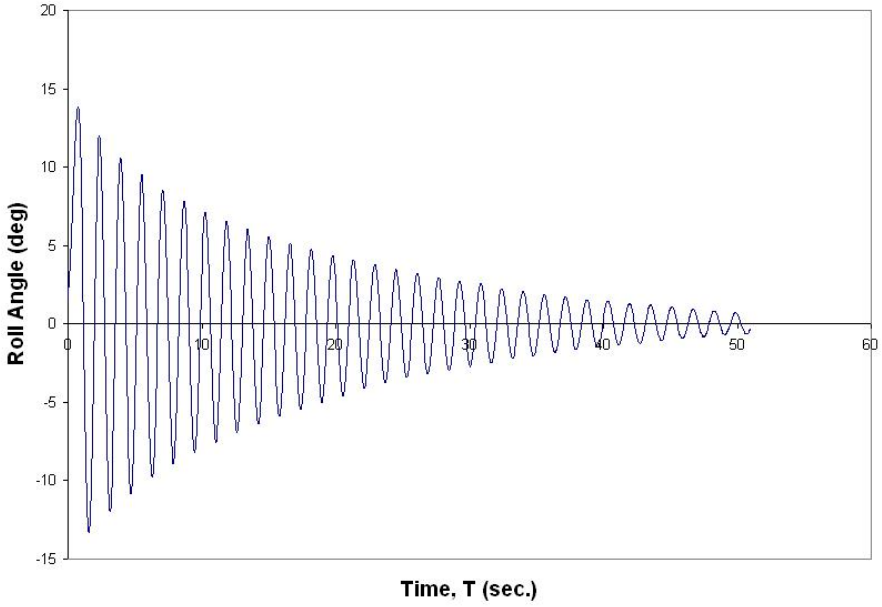

Fig. 4.4: Typical free decay test record

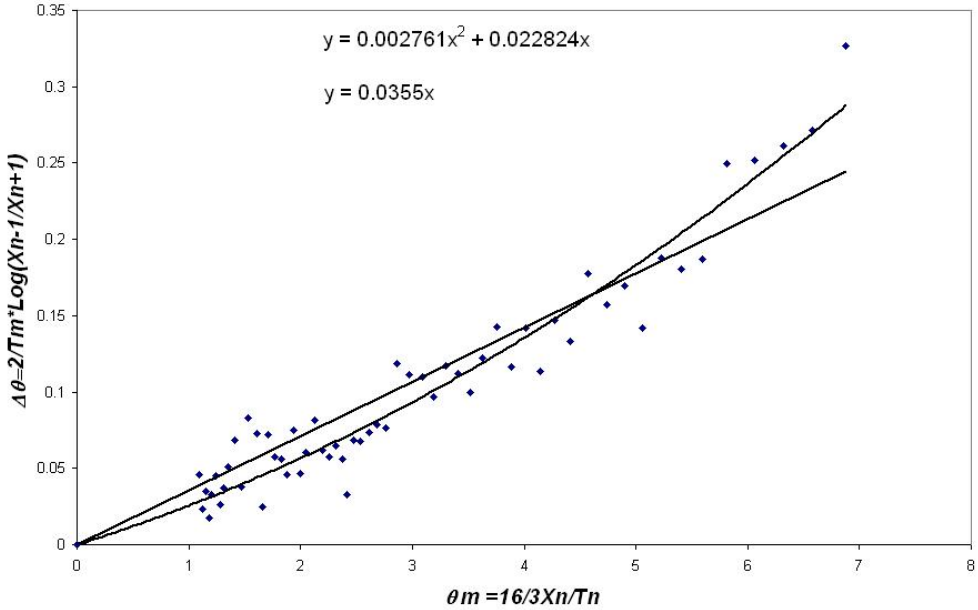

Fig. 4.5: Analysis of the free decay test

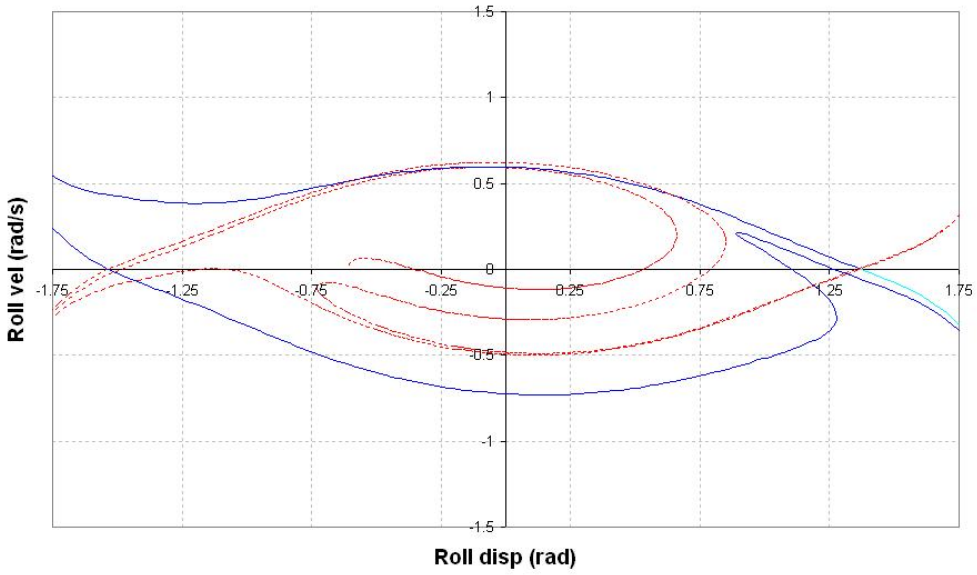

Fig. 4.6: DDG51 Poincaré map, 11.4 ft wave and low damping-numerical

damping) at the forcing frequency have been taken from a linear ship motions analyses performed on the same unit. The quadratic damping coefficient is estimated from sallying experiments performed on a scaled model and observing the roll decay tests in the University of New Orleans (UNO) Tow Tank facility (see Figure 4.4 and Figure 4.5). It was found that by adjusting the orientation of the rudder angle in the model, two generic cases for the damping resulted viz. a higher estimate when the rudders were zero degrees astern and a lower estimate when the rudders were aligned ninety degrees astern. The results are shown for the low damping case which illustrates the importance of damping as manifold intersections were already observed in the Poincaré maps (see Figure 4.6) when analyzed numerically for the system parameters shown in Table 4.2.

An essential and interesting aspect and also noted by previous studies (Falzarano, 1990, Falzarano & Vishnubhotla, 2000, Hsieh et.al, 1994) is that for a given wave amplitude, under periodic forcing, the qualitative structure of the manifolds changes (when they begin to intersect) for a particular initial phase of the forcing function (or t_0, see Chapter 3) given specifically by the zeroes of the Melnikov function. Analogously this is also depicted by observing a similar change in the two dimensional (2 D) phase projection of the manifolds, as t_0 is slowly varied, just prior to and after a possible manifold intersection.

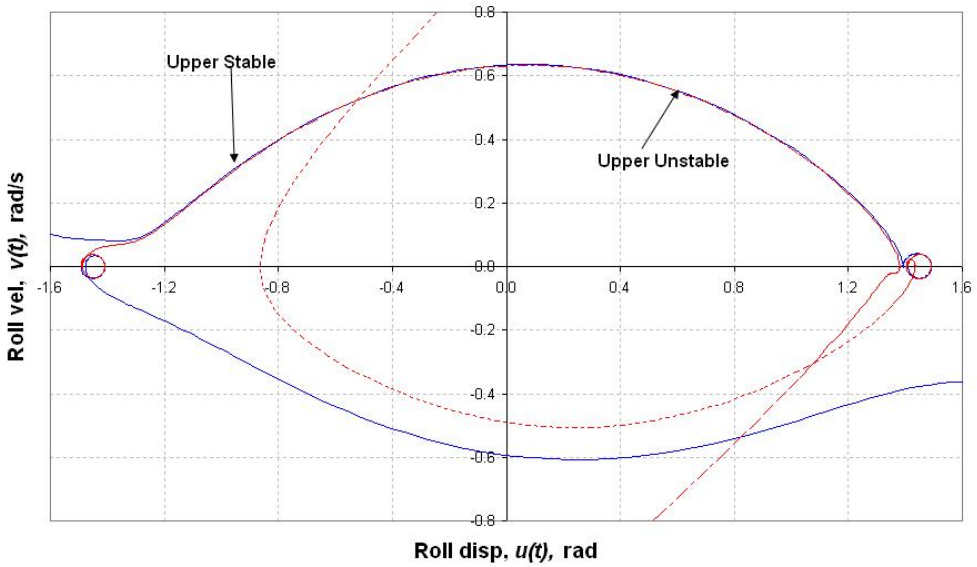

Fig. 4.7: DDG51 perturbation manifold solutions for $t_0 = 0.40$

If the unstable manifold remains inside the stable manifold then the situation is still bounded and considered safe i.e initial conditions inside the safe basin will remain stable. However if the stable manifold is inside the unstable manifold then any solution starting around the basin boundary will lead to an unstable situation and may result in capsize. This is illustrated in Figures 4.7 and Figure 4.8 where for $t_0 = 0.40$ the upper unstable manifold remains inside the upper stable while for $t_0 = 0.35$ the opposite happens. Hence the manifolds ought to intersect at some value $0.35 < t_0 < 0.40$ by continuity (Vakakis, 1993, Rand, 1994). A similar situation is repeated for the lower manifolds in the range $1.60 < t_0 < 1.65$ and is shown in Figure 4.9 and Figure 4.10.

In fact a straight forward calculation (see Chapter 3) using the perturbation solutions suggests that the exact values, when the upper (stable and unstable) and lower (stable and unstable) solutions begin to intersect, are given by $t_{01} = 0.37$ and $t_{02} = 1.625$ respectively. This is also verifiable by when the Melnikov function attains simple zeroes for the following two scenarios for the intersection of upper and the lower manifold solutions respectively:

$$M(t_{01}) = \frac{2}{k}\gamma\ \pi\ \Omega\ \frac{\cos(\Omega t_{01})}{\sinh\frac{\Omega\pi}{\sqrt{2}}} - \frac{2\sqrt{2}}{3k}\delta - \frac{8}{15}\ \frac{\delta_q}{k^{1.5}}\ =\ 0 \tag{4.1}$$

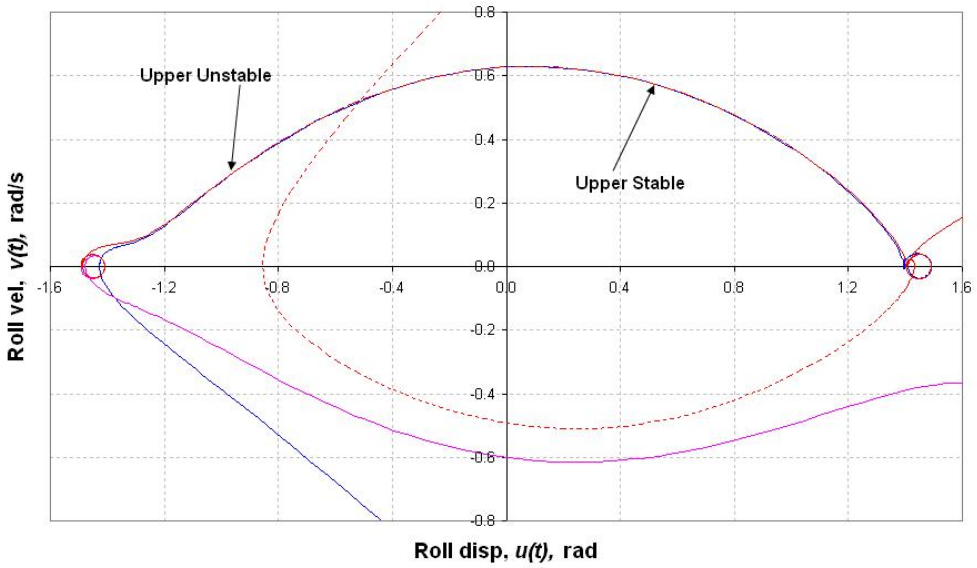

Fig. 4.8: DDG51 perturbation manifold solutions for $t_0 = 0.35$

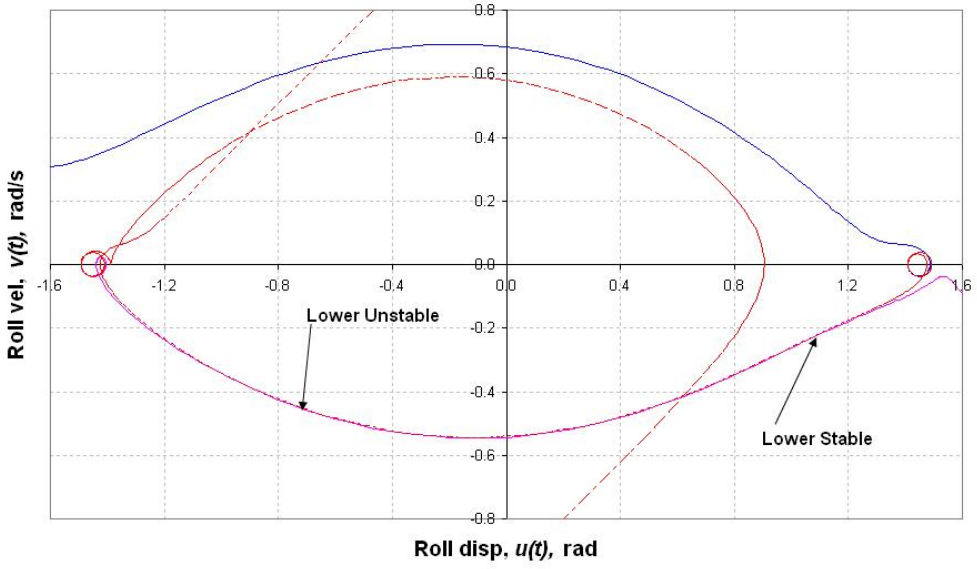

Fig. 4.9: DDG51 perturbation manifold solutions for $t_0 = 1.60$

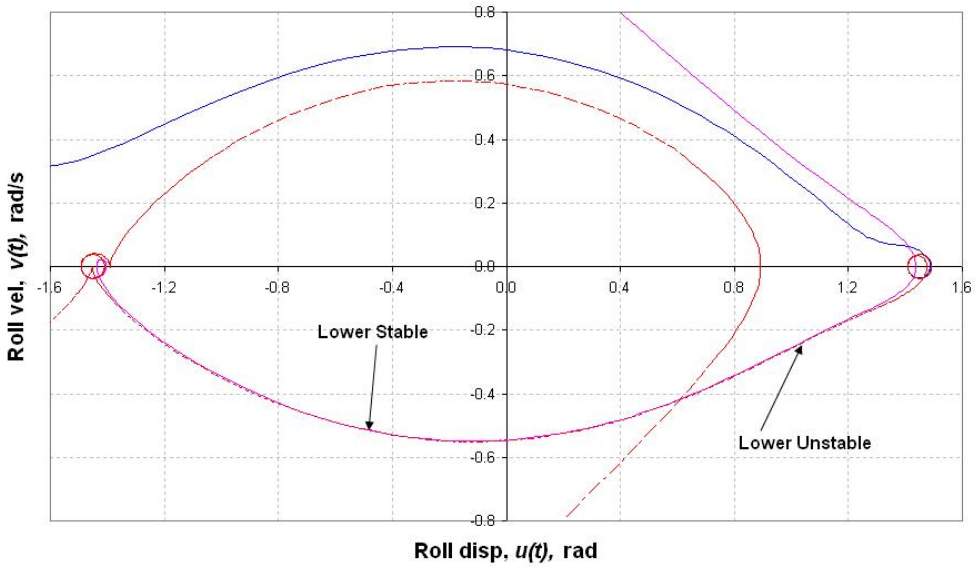

Fig. 4.10: DDG51 perturbation manifold solutions for $t_0 = 1.65$

$$M(t_{02}) = -\frac{2}{k}\gamma\ \pi\ \Omega\ \frac{\cos(\Omega t_{02})}{\sinh\frac{\Omega\pi}{\sqrt{2}}} - \frac{2\sqrt{2}}{3k}\delta - \frac{8}{15}\ \frac{\delta_q}{k^{1.5}}\ =\ 0 \tag{4.2}$$

4.3 T-AGOS safe basin using perturbation solution (pseudo random forcing)

The analytical solution approach utilized herein to track the critical stable manifolds (or the capsize boundaries) of a floating unit has been applied to an extensive array of vessels ranging in size from a small crab vessel such as the *Patti*-B ($\sim$ 50 ft in length) to a Mobile Offshore Base (MOB) unit ($\sim$ 1000 ft). Results for these vessels which have also included a tanker based FPSO and an Offshore Supply Vessel (OSV), (the T-*AGOS*) can be found in Vishnubhotla et.al. (2000, 2004).

The current section presents (Figures 4.14 through 4.20) some of the recent results obtained for an OSV (the T-*AGOS*) showing the projected phase plane (PPP) of the stable manifolds or the safe basin for (the unstable manifolds were found to be within the stable manifolds and are not shown in the phase plane projections)

- Two different sea states - Sea State 3 (Wind Speed = $U_W = 9 \text{fts}^{-1}$) and Sea State 7 (Wind Speed = $U_W = 32.8 \text{fts}^{-1}$);
- Varying levels of damping (with and without bilge keels (B-K) as well as using $B_{44q}(\omega) = 0$

Parameter	Units	Dimensional Value
Length of the vessel, L	ft	215.70
Displacement, Δ	lb	4425000.00
Linear restoring arm, C_1	ft	4.680
Nonlinear restoring arm, C_3	ft	2.793
Linear natural frequency, ω_n	rad/s	0.572
Hydrodynamic mass, $(I_{44} + A_{44}(\omega))$	slug-ft^2	39783000.00
Linear damping, $B_{44}(\omega)$	slug-ft^2-s^{-1}	38000000.00
Nonlinear damping, B_{44q}	slug-ft^2	1405400.00

Tab. 4.3: Parameters for the offshore supply vessel T-*AGOS*

(no viscous damping) in some cases.

Finally a typical three dimensional extended phase space plots depicting the lower stable and upper unstable manifold orbits are also shown for the two sea states.

4.4 Manifold solutions of DDG51 for CCM and CIM approximations

As a comparison to the periodic results reported earlier for the traditional naval hull destroyer, DDG51, results for the low damping case as previously explained are presented here. The forcing function is computed as a Fourier decomposition of a 2 parameter (significant wave height and frequency) Bretschneider sea spectrum given by the description in equation (2.22) of Chapter 2. The roll moment transfer function for this vessel as obtained by running a linear ship motions computer program (Beck & Troesch, 1989) is shown in Figure 4.22 while the stable and unstable manifold solutions for sea states 2 and 5 are shown in Figure 4.23 and Figure 4.24 respectively.

The solutions obtained using the convolution integral to capture the memory dependent hydrodynamics is referred to as the CIM, while the one using constant coefficients is denoted as CCM. A comparison of the stable manifolds due to the two methods is shown in Figure 4.25 for

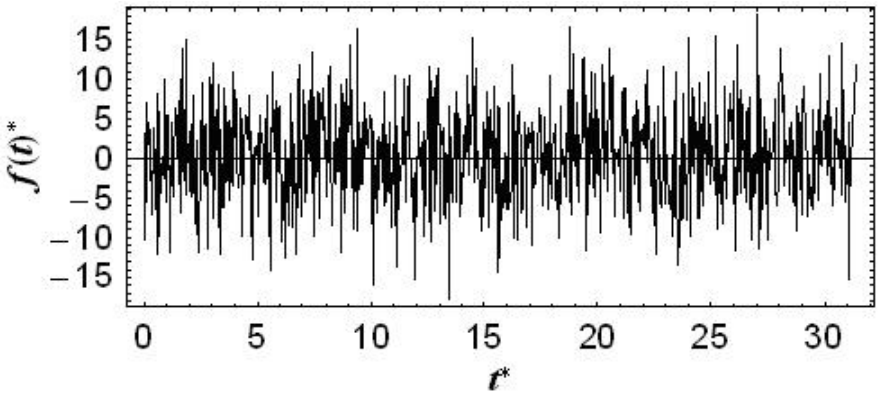

Fig. 4.11: T-*AGOS* typical roll moment excitation time history

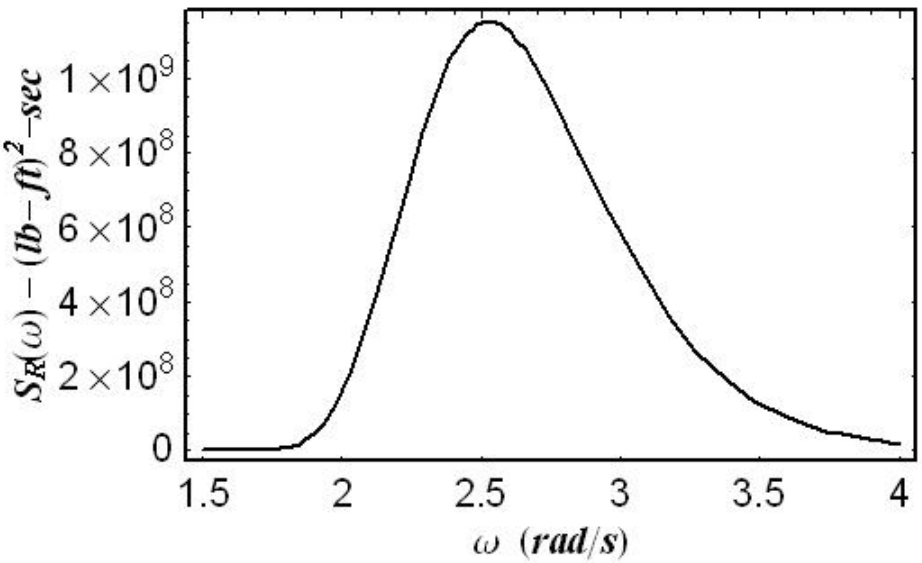

Fig. 4.12: T-*AGOS* roll moment spectra for Sea State 3

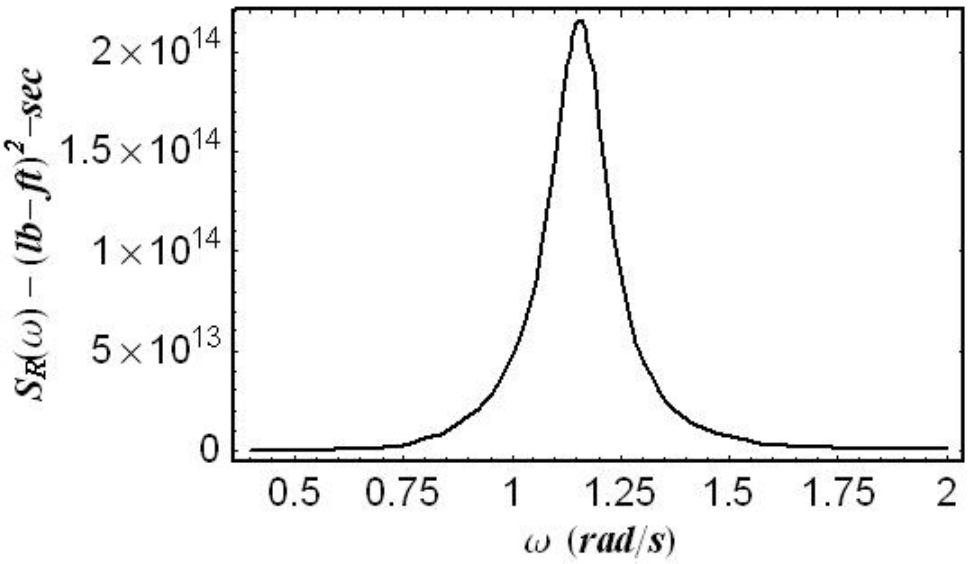

Fig. 4.13: T-*AGOS* roll moment spectra for Sea State 7

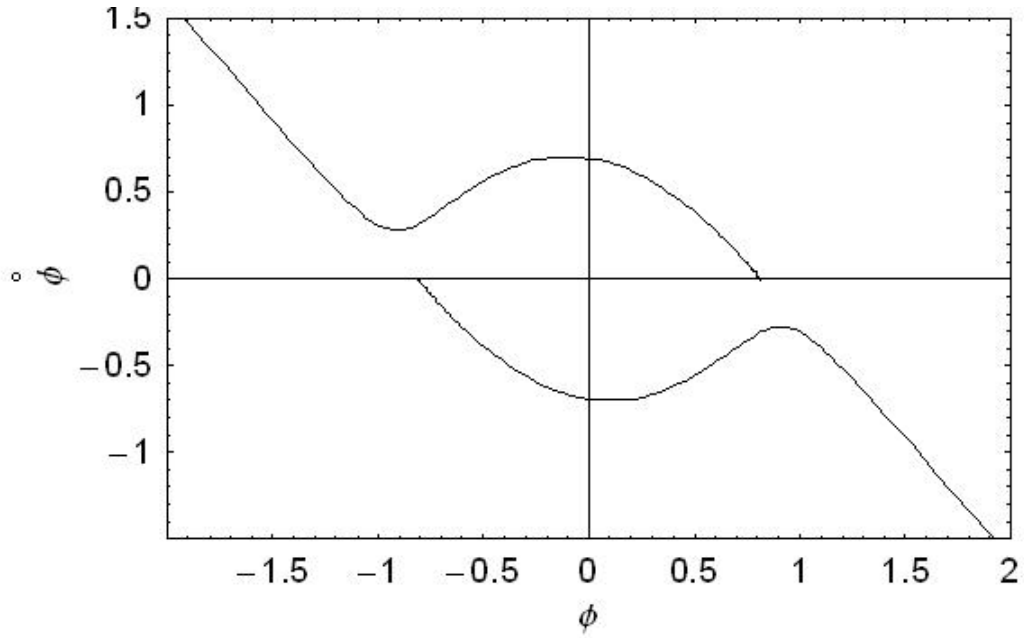

Fig. 4.14: T-*AGOS* safe basin, Sea State 3, w/o B-K, $B_{44q} = 0$

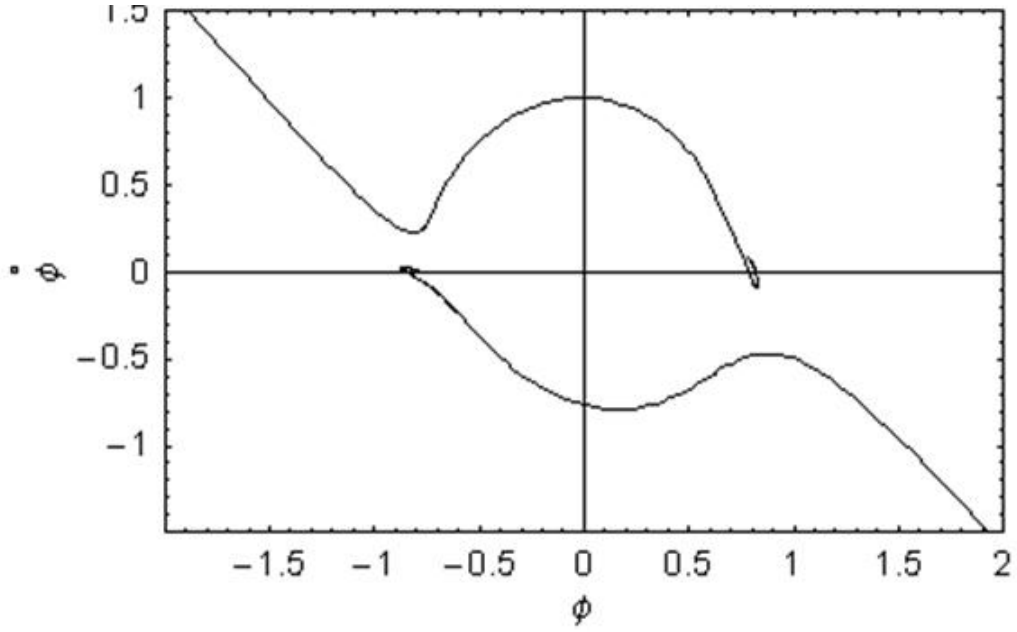

Fig. 4.15: T-*AGOS* safe basin, Sea State 7, w/o B-K, $B_{44q} = 0$

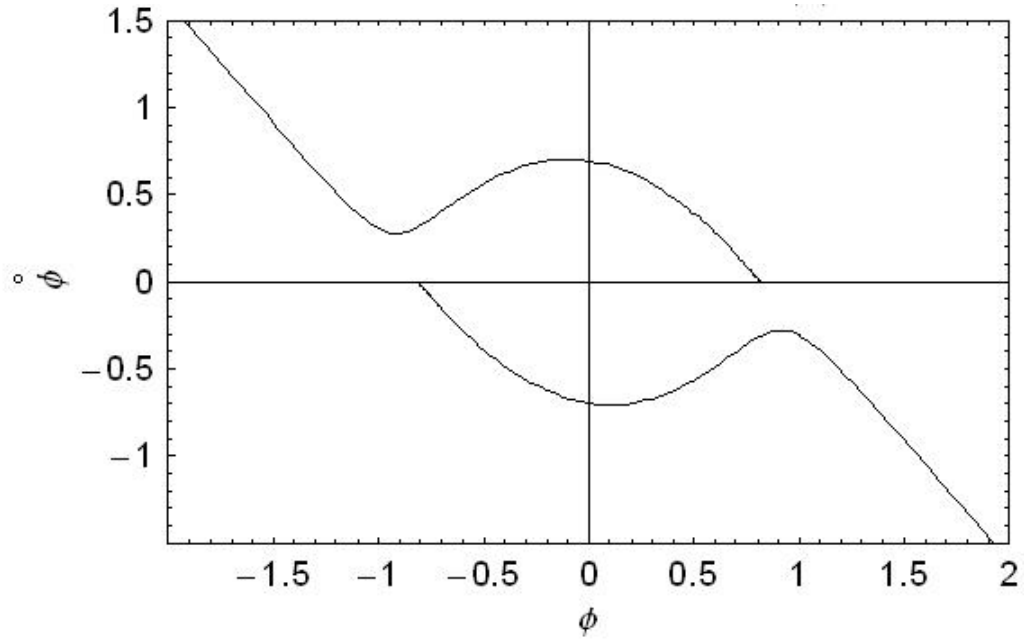

Fig. 4.16: T-*AGOS* safe basin, Sea State 3, w/o B-K, $B_{44q} \neq 0$

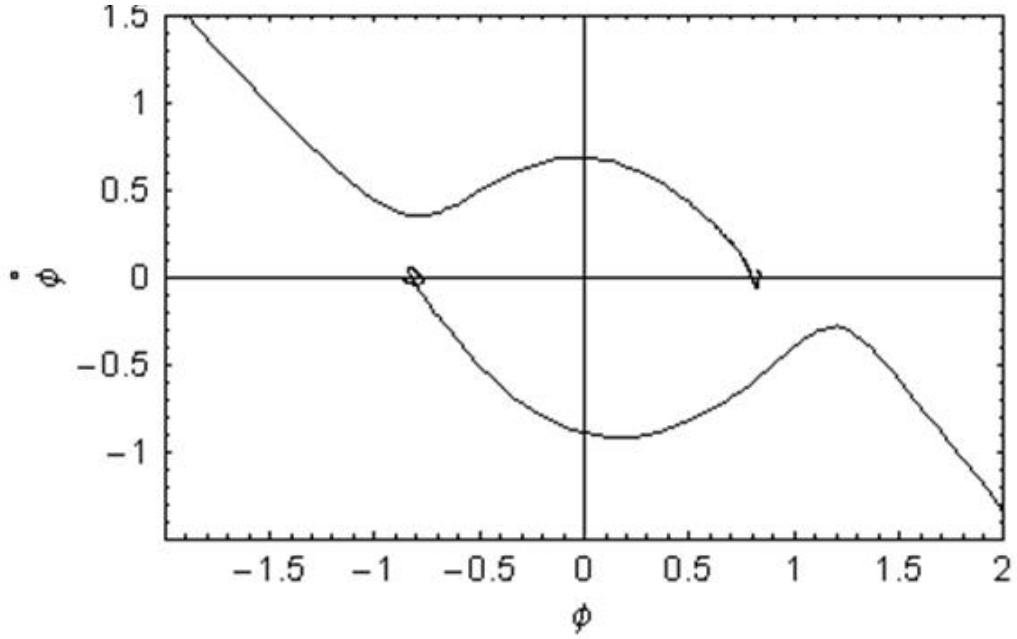

Fig. 4.17: T-*AGOS* safe basin, Sea State 7, w/o B-K, $B_{44q} \neq 0$

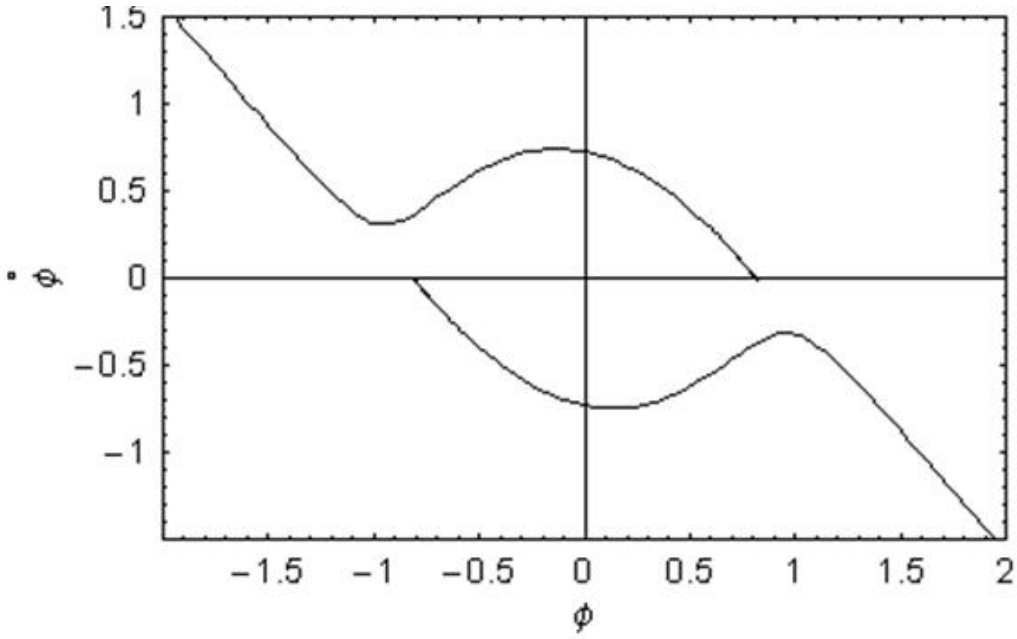

Fig. 4.18: T-*AGOS* safe basin, Sea State 3, w/i B-K, $B_{44q} \neq 0$

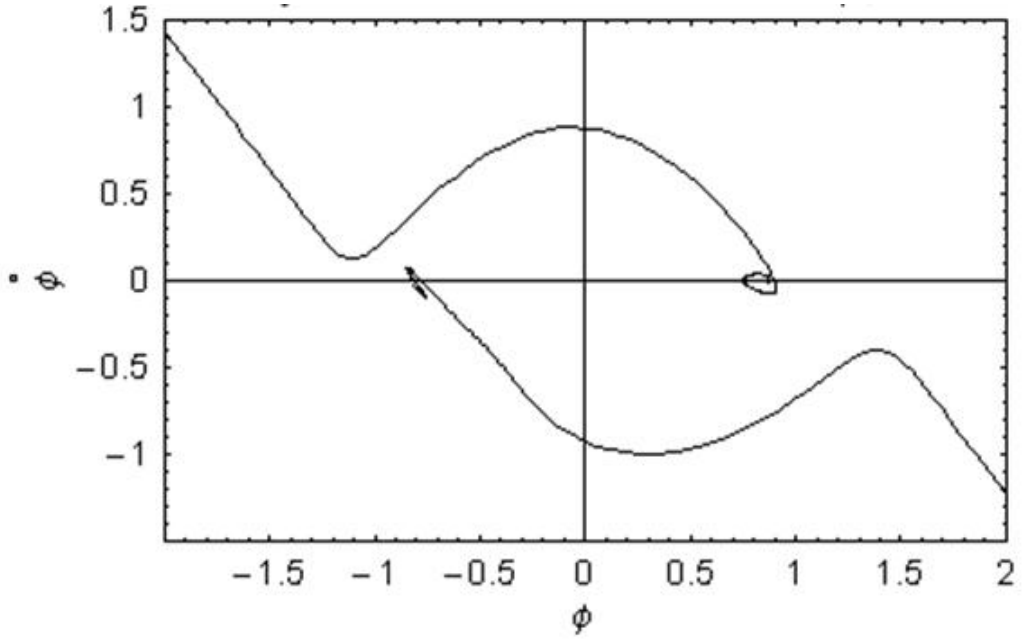

Fig. 4.19: T-*AGOS* safe basin, Sea State 7, w/i B-K, $B_{44q} \neq 0$

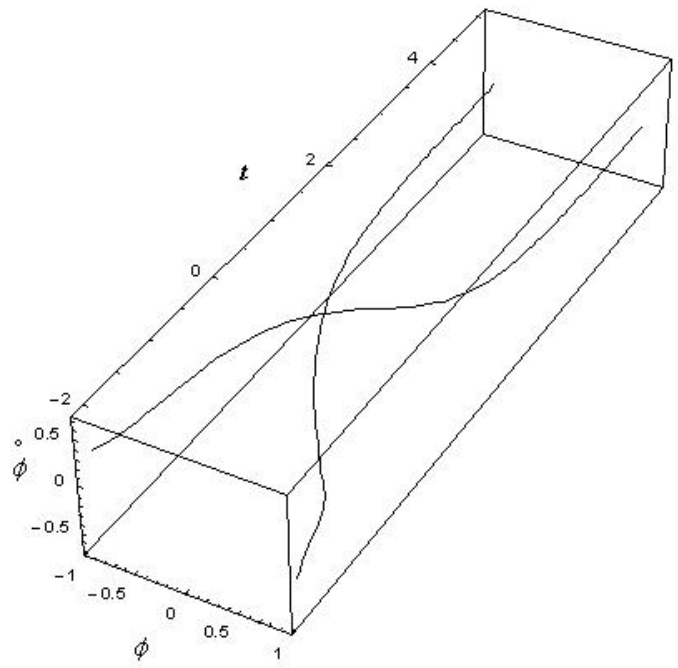

Fig. 4.20: Extended phase space showing upper unstable and lower stable solutions, Sea State 3, w/o B-K

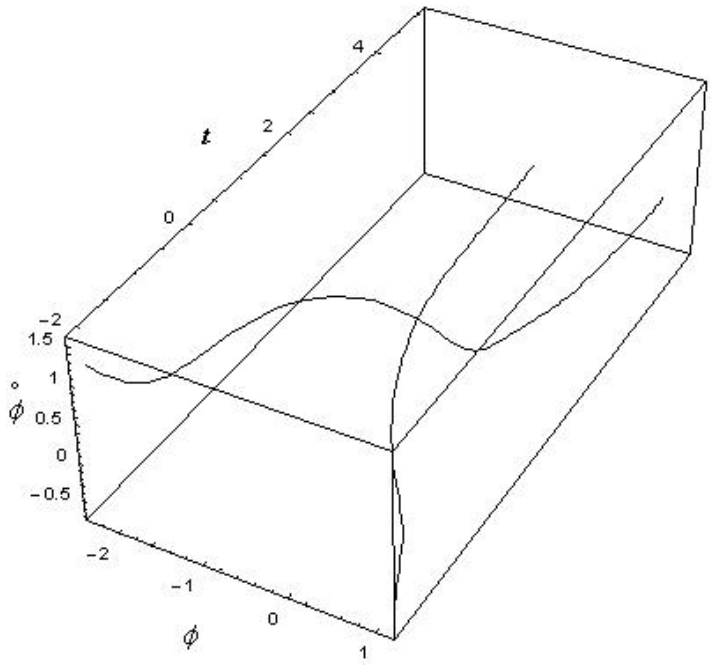

Fig. 4.21: Extended phase space showing upper unstable and lower stable solutions, Sea State 7, w/o B-K

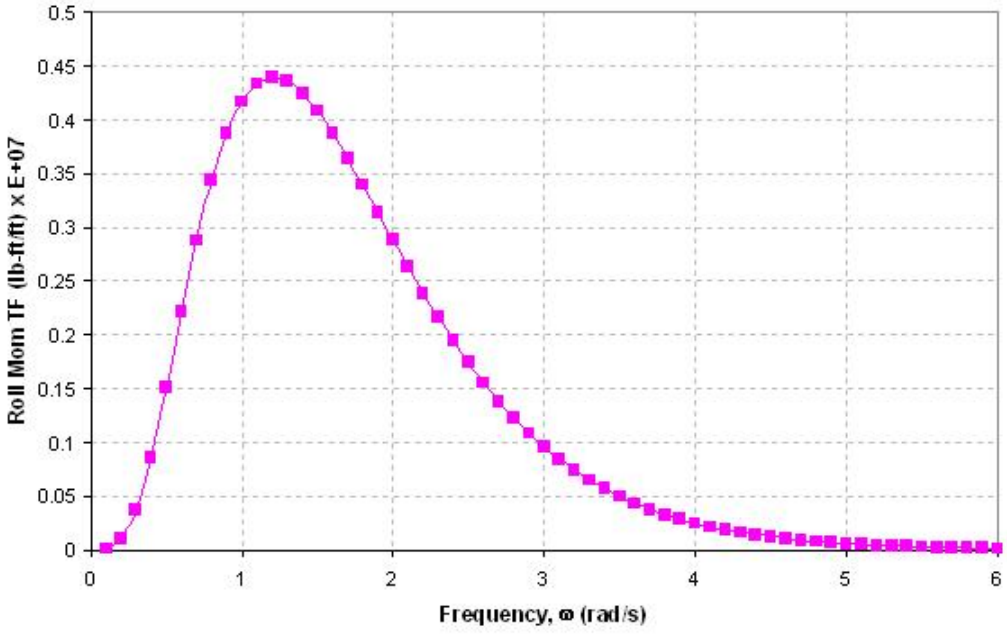

Fig. 4.22: DDG51 roll moment transfer function (RAO)

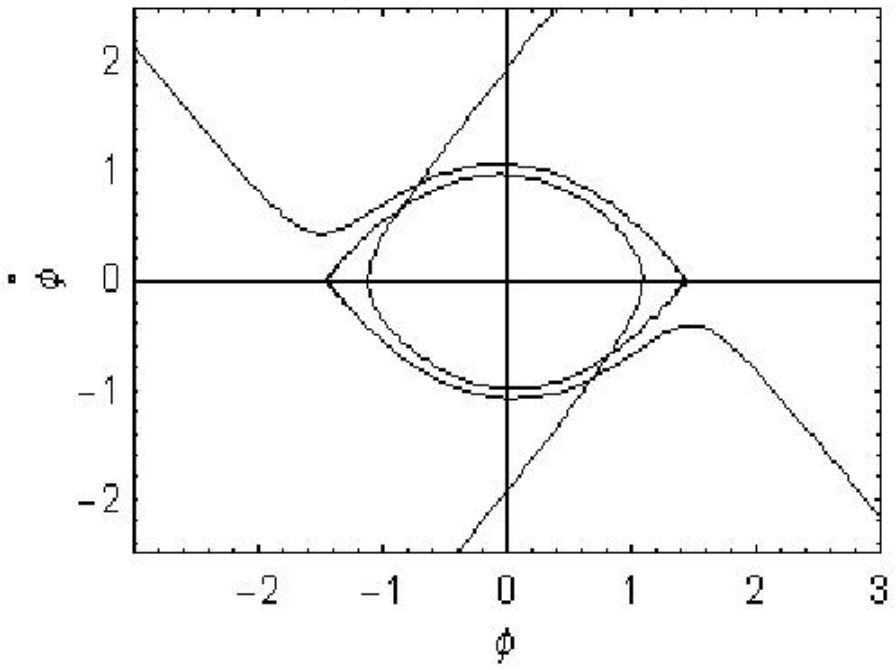

Fig. 4.23: DDG51 Projected Phase Plane for Sea State 2, [Hs, Tp] = [2.9 ft, 7.5s]

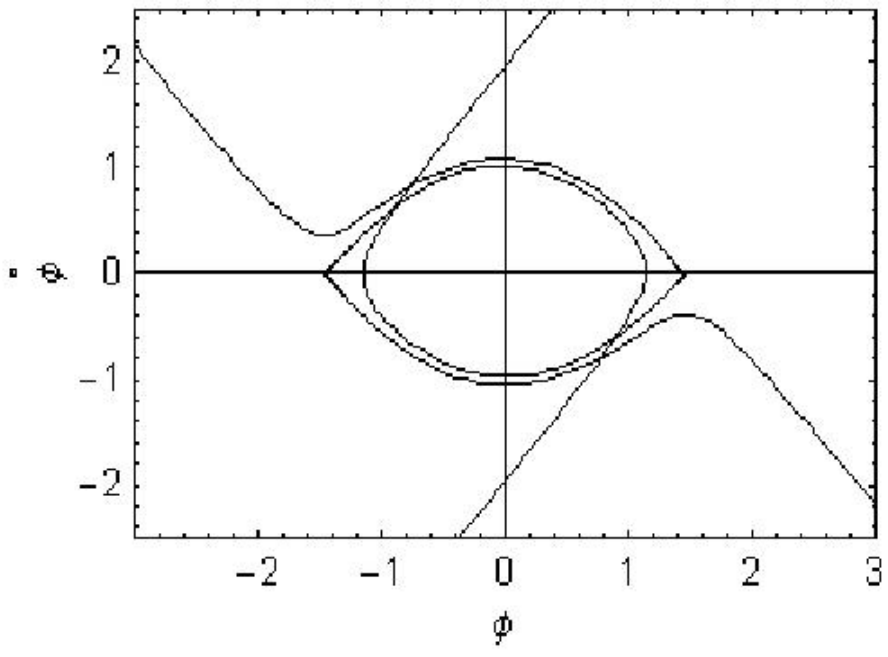

Fig. 4.24: DDG51 Projected Phase Plane for Sea State 5, [Hs, Tp] = [10.7 ft, 9.7s]

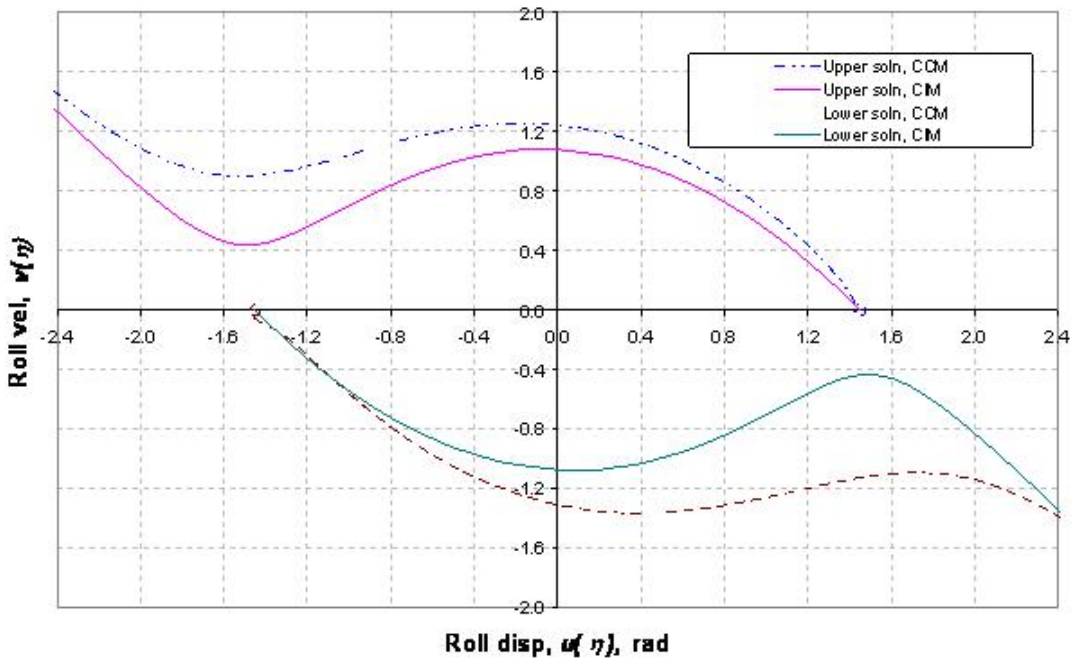

Fig. 4.25: Comparison of Stable manifold solutions for Sea State 2 CCM (dotted) and CIM (solid)

a Sea State 2 seaway intensity. Similar to the results shown earlier for periodic forcing, the stable and the unstable manifold solutions of the saddle points at the angles of vanishing stability can be calculated for different initial phase values of t_0. For a sufficiently small forcing case (Sea State 2) where the unstable manifolds lie well within the stable manifolds, Figure 4.26 and Figure 4.27 show the stable and unstable manifolds respectively for a case of five initial phases.

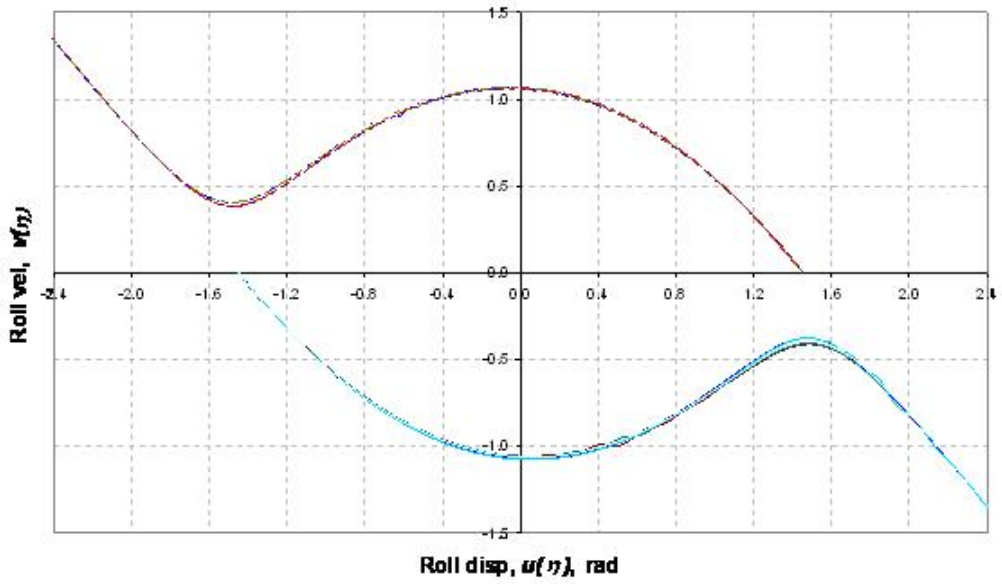

Fig. 4.26: Stable manifolds for 5 initial phases $t_0 = 0.7025$, 2.396, 4.1456, 0.6085 and 5.541

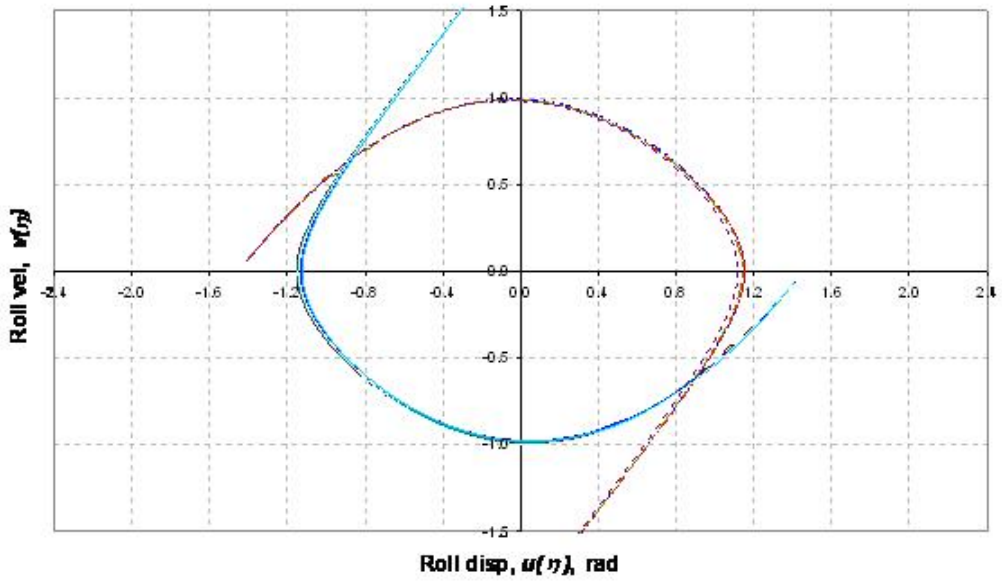

Fig. 4.27: Unstable manifolds for 5 initial phases $t_0 = 0.7025$, 2.396, 4.1456, 0.6085 and 5.541

5. CONCLUSIONS AND FUTURE WORK

5.1 A practical technique to analyze the problem of ship capsize

Using global perturbation or geometric method, an analysis tool from the theory of dynamical systems coupled with a mathematical solution procedure for ordinary differential equations, a technique to analyze the global behavior of ship rolling in a realistic seaway is considered. Semi-analytic expressions for certain specific solutions called the invariant manifolds accurate up to the first order are calculated and their usefulness discussed under a random forcing excitation due to a given seaway intensity. The approach utilized herein can accommodate the exact nonlinear roll hydrostatics away from the zero roll angle as well as the nonlinear viscous roll damping. While closed form analytic solutions have been determined for a cubic approximation to the hydrostatic restoring moment curve, the solution methodology is applicable to arbitrary higher order approximations to the restoring curve.

While the technique is applied to cases with no static bias (upright equilibrium at zero roll angle) it can be extended to cases with static bias (upright equilibrium at a nonzero roll angle). Two models called the constant coefficient and the convolution integral have been developed to study the nature of the solutions without and with the impulse response functions, that are used to assess the effect of the memory dependent hydrodynamics. It has been seen that the effect of the amount of damping dramatically affects the results. Hence an accurate estimate of the linear and nonlinear damping is crucial in studying the nature of the solutions. For weakly under damped systems, as the forcing increases, the nature of the stable and unstable manifold solutions qualitatively changes with different initial time phases and the difference is more pronounced when the forcing reaches a critical value and a critical time phase. In this respect the methodology presented herein is equivalent to the Melnikov approach used by other research groups.

5.2 An alternative to Melnikov technique in ship system dynamical studies

It has been observed by several research groups that the critical large amplitude in roll motion as experienced by a ship due to a combination of a sufficiently large wave excitation in the presence of small or very small damping is closely related to the behavior of the invariant manifold solutions of the saddle points at the angles of vanishing stability. Furthermore the measure of the distance function between the manifolds called the Melnikov function and the measure of its positive part has been correlated to the likelihood of an initial condition escaping from the safe region. Initial work on the Melnikov theory for single degree of freedom roll equation of motion has been considered in detail for harmonic excitation (Falzarano, 1990, 1992). Frey and Simiu (1993) were the first to develop a generalized Melnikov treatment to stochastic excitation due to random noise on second order dynamical systems. Two other independent groups, Lin & Yim, (1995) and Hsieh et.al (1994) applied the generalized Melnikov function using slightly different formulations to study the chaotic roll response and the capsize criteria for ships due to random excitation.

While many previous studies have analyzed the nonlinear dynamical systems without explicitly determining the perturbed solutions, the approach suggested herein calculates explicitly the semi-analytic solution up to the first order. The nature of how the manifold solutions evolve for a given forcing and damping can be clearly illustrated and understood with the solutions developed herein. It was however observed that up to the first order the separation of the manifolds do not explicitly depend on the perturbed solutions. In fact the distance function computed using the solutions from the method developed herein turned out to be identical to the distance function as determined from the Melnikov function and hence this method can be can be used as an alternative in lieu of a Melnikov approach.

5.3 An aid to numerical simulations and methods

One of the advantages of knowing these solutions analytically in case of periodic forcing is the straightforward estimation of the saddle-type periodic orbits or fixed points which by virtue of being unstable are very difficult to estimate numerically or analytically. An approximate knowledge of the manifold solutions apriori can be a useful criteria for a good initial guess for any numerical program or simulation method that attempts to locate the unstable saddle type orbits.

5.4 An intermediate step to higher order approximations

The known first order and the zeroth order solutions determined herein can be useful quantities in future studies that focus on higher order approximations to the manifold solutions or to the distance function between the manifolds. A key feature of the Melnikov technique to date has been to estimate the measure of the distance function to the first order by just knowing the zeroth order solutions to the manifold. However if one needs to calculate the distance measure and the nature of its evolution with forcing and damping with greater accuracy, the current practice of using the Melnikov technique accurate up to the first order may not be sufficient. For Melnikov function accurate up to the second order of approximation, both the zeroth and the first order solutions as outlined in the solution procedure herein would prove useful.

REFERENCES

Beck, R. F. and Troesch, A. W. *Department of Naval Architecture and Marine Engineering Students Documentation and Users Manual for the Computer Program SHIPMO*, Report No. 89-2, Ann Arbor, MI. (1989).

Belenky, V. L, Degtyarev, A. B. and Boukhanovsky, A. V. Probabilistic qualities of Nonlinear Stochastic Rolling. *Ocean Engineering*. 25:1-25. (1998).

Belenky, V. L. Probabilistic approach to intact ship stability standards. *SNAME Transactions*. 108:123-146. (2000).

Biran, A. *Ship Hydrostatics and Stability*. Butterworth-Heinemann, an imprint of Elsevier. (2003).

Cardo, A., Francescutto, A. and Nabergoj, R. Ultraharmonics and Subharmonics in the Rolling Motion of a Ship: Steady State Solution. *International Shipbuilding Progress*. 28: 233-25. (1981).

Chakrabarti, S. K. *Hydrodynamics of Offshore Structures*. Computational Mechanics Publications. (1994).

Cummins, W. E. The impulse response function and ship motions. *Schiffstechnik*. 47: 101-109. (1962).

Er, G-K Consistent method for PDF solutions of random oscillators. *Journal of Engineering Mechanics*. 125: 443-447. (1999).

Er, G-K and Iu, V. P Probabilistic solutions to nonlinear random ship roll motion. *Journal of Engineering Mechanics*. 125: 570-574. (1999).

Er, G-K The probabilistic solutions to nonlinear random vibrations of MDOF systems. *Journal of Engineering Mechanics*. 67: 355-359. (2000).

Faltinsen, O. M. *Sea Loads on Ships and Offshore Structures*. Cambridge University Press. (1990).

Falzarano, J. M. *Predicting complicated Dynamics leading to Vessel Capsizing*. Univ. of Michigan, Ann Arbor. (1990).

Falzarano, J., Shaw, S. and Troesch, A. Application of Global Methods for Analyzing Dynamical Systems to Ship Rolling Motion and Capsizing. *International Journal of Bifurcation and Chaos*. 2 : 101-116. (1992).

Falzarano, J., Esparza, I. and Taz Ul Mulk, M. A combined steady state and transient approach to study large amplitude ship rolling motion and capsizing. *Journal of Ship Research*. 39: 213-224. (1995).

Falzarano, J, Kalyan, U, Rodrigue, W. and Vassilev, R. MOB Transit Draft Stability and Dynamics: An Analytic Study. *Very Large Floating Structures, VLFS*, (1999).

Falzarano, J., Cheng, J. and Rodrigues., W. Transit draft heave and pitch motion analysis of the mobile offshore base (MOB) using reverse MI/SO techniques. *Transactions of the ASME*. 126:16-25. (2004).

Falzarano, J., Vishnubhotla, S and Juckett, S. Combined Steady State and Transient Analysis of a Patrol Vessel as Affected b Varying Amounts of Damping and Periodic and Random Wave Excitation, *OMAE 2005 Conference*. (2005).

Francescutto, A. On the nonlinear motions of ships and structures in narrow band sea. *Dynamics of Marine Vehicle and Structures in Waves, Elsevier Science*, : 291-303. (1991).

Francescutto, A. Nonlinear ship rolling in the presence of narrow band excitation. *Nonlinear Dynamics of Marine Vehicles, ASME, DSC*. 51: 93-102. (1993).

Francescutto, A. On the statistical distribution of stochastic nonlinear rolling. *Risk and Reliability in Marine Technology*. C. Guedes-Soares (Editor), Balkema.A.A. 107-116. (1998).

Francescutto, A. and Naito, S. Large amplitude rolling in a realistic sea. *8th International conference on Stability of Ship and Ocean Vehicles*. 495-505. (2003).

Frey, M. and Simiu, E. Noise-induced chaos and phase space flux. *Physica D* 63: 321-340. (1993).

Frey, M. and Simiu, E. Melnikov processes and noise induced exits from a well. *Journal of Engineering Mechanics*.122:263-270. (1996).

Flower, J. O. A Perturbational Approach to Non-Linear Rolling in a Stochastic Sea. *International Shipbuilding Progress*. 23: 209-212. (1976).

Guckenheimer, J. and Holmes, P. *Non-Linear Oscillations, Dynamical Systems, and Bifurcations of Vector Fields*. Springer, New York. (1983).

Hasselman, K. On the Nonlinear Ship Motions in Irregular Seas. *Journal of Ship Research*. 10: 64-68. (1966).

Holappa, K. W. and Falzarano, J. M. Application of extended state space to nonlinear ship rolling. *Ocean Engineering*, 26, 227-240. (1999)

Hsieh, S. R., Shaw, S. W. and Troesch, A. W. A Predictive Method for Vessel Capsize in Random Seas. *Nonlinear Dynamics of Marine Vehicles*. ASME, DSC-51 (OMAE-1). (1993).

Hsieh, S. R., Troesch, A. W. and Shaw, S. W. A Nonlinear Probabilistic Method for Predicting Vessel Capsizing in Random Beam Seas. *Proceedings of the Royal Society of London.* A, 446: 195-211. (1994).

Huang., X. The investigation of the safe basin erosion under the action of the random waves. 8^{th} *International conference on Stability of Ship and Ocean Vehicles.* 539-549. (2003).

Huang., X. , Zhu, X. Some discussions about the probability of capsize of a ship in random beam waves. *Proceed. of* 5^{th} *International Workshop on Stability and Operational safety of Ships.*4.7.1-4.7.8. (2003).

Jiang, C., Troesch, A. W. and Shaw, S. W. Highly Nonlinear Rolling Motion of Biased Ships in Random Beam Seas. *Journal of Ship Research.* 40: 125-135. (1996).

Jiang, C., Troesch, A. W. and Shaw, S. W. Capsize Criteria for Ship Models with Memory-Dependent Hydrodynamics and Random Excitation. *Philosophical Transactions of the Royal Society.* 358: 1761-1791. (2000).

Korpus, R and Falzarano, J. Prediction of Viscous Ship Roll Damping by Unsteady Navier-Stokes Techniques, *Journal of Offshore Mechanics and Arctic Engineering (OMAE), ASME.* (1997)

Kota, R, Falzarano, J. and Vakakis, A. Survival Analysis of Deep-water Floating Offshore Platform about its critical its Axis: including Coupling. *Journal of International Society of Offshore and Polar Engineers.* (1998).

Lin, H. and Yim, S. C. S. Chaotic roll motion and capsize of ships under periodic excitation with random noise. *Applied Ocean Research* 17: 185-204. (1996).

Lin, H. and Yim, S. C. S. Analysis of a Nonlinear System Exhibiting Chaotic, Noisy Chaotic, and Random Behaviors. *Journal of Applied Mechanics.* 63: 509-516. (1996).

Lin, H. and Yim, S. C. S. Stochastic analysis of a SDOF nonlinear experimental moored system using an independent-flow-field model. *Journal of Engineering Mechanics.* 130: 161-169. (2004).

Lin, Y. K. *Probabilistic Theory of Structural Dynamics.* McGraw-Hill, New York. (1967)

McRobie, F.A. and Thompson, J. M.T. Lobe dynamics and the escape from a potential well. *Proceedings of the Royal Society of London.* A435: 659-672. (1991).

Melnikov, V. K. On the stability of the center for time periodic perturbations. *Transactions of the Moskow Mathematical Society.* (1962).

Moshchuk, N. K, Ibrahim, R. A., Khasminskii, R. Z. and Chow, P. L. Ship Capsizing in Random Sea Waves and the Mathematical Pendulum. *IUTAM.* (1996).

Nayfeh, A. H. and Khdeir, A. A. Nonlinear Rolling of Biased Ships in Regular Beam Waves. *International Shipbuilding Progress.* 3: 84-93. (1986).

Ochi, M. K. *Ocean Waves, the Stochastic Approach.* Cambridge University Press. (1998).

Parker, T. S. and Chua, L. O. *Practical Numerical Algorithms for Chaotic Systems.* Springer-Verlag. (1989)

Rand, R. H. *Topics in Nonlinear Dynamics with Computer Algebra. Volume 1*, Computation in Education: Mathematics, Science and Engineering. Gordon and Breach Science Publishers. (1994)

Rice, S. O. Mathematical Analysis of Random Noise. *Bell Syst. Tech. Journal*, 23, 282-332. (1944)

Roberts, J. B. Estimation of Non-Linear Ship Roll Damping from Free-Decay Data. *Journal of Ship Research* 29: 127-138. (1985).

Roberts, J. B. A Stochastic Theory of Nonlinear Ship Rolling in Irregular Seas. *Journal of Ship Research.* 26: 229-245. (1986).

Roberts, J. B. Response of an Oscillator with Non-Linear Damping and a Softening Spring to Non-White Random Excitation. *Probabilistic Engineering Mechanics.* 1: 40-48. (1986).

Roberts, J. B. Ship rolling and capsize in irregular seas. *Risk and Reliability in Marine Technology.* Balkema, A. A. 46: 117-136. (1998).

Roberts, J. B. First passage probabilities for randomly excited systems: Diffusion methods. *Probabilistic Engineering Mechanics.* 1: 66-81. (1986).

Ross, S. L. *Differential Equations.* Third Edition, John Wiley and Sons. (1984).

Senjanovic, I., Cipric, G and Parunov, J. Survival analysis of fishing vessels rolling in rough seas. *Philosophical Transactions of the Royal Society* 358: 1943-1965. (2000).

Soliman, M. S. Analysis of Ship Stability based on Transient Motions. 4^{th} *International Conference on Stability of Ship and Ocean Vehicles.* 183-190. (1990).

Soliman, M. S. and Thompson, J. M. T. Stochastic penetration of smooth and fractal basin boundaries under noise excitation. *Dynamics and Stability of Systems.* 5: 281-298. (1990).

Thompson, J. M. T. Designing against capsize in beam seas: Recent advances and new insights. *Applied Mechanics Review.* 50: 307-324. (1997).
Vakakis, A.. Splitting of Separatrices of the Rapidly Forced Duffing Equation. *Nonlinear Vibrations*, ASME Vibrations Conference, September. (1993).

Vassilopoulos, C. Ship Rolling in Random Beam Seas with Nonlinear Damping and Restoration. *Journal of Ship Research.* 15: 289-294. (1971).

Virgin, L. N. The Nonlinear Rolling Response of a Vessel including Chaotic Motions leading to Capsize in Regular Seas. *Applied Ocean Research.* 9: 89-95. (1987).

Vishnubhotla, S., Falzarano, J. M. and Vakakis, A. A New Method to Predict Vessel/Platform Capsizing in a Random Seaway. 3^{rd} *International Conference on Computational Stochastic Mechanics*. 497-502. (1998).

Vishnubhotla, S., Falzarano, J. M. and Vakakis, A. MOB Platform Large Amplitude Dynamics in a Random Seaway. 9^{th} *International Society of Offshore and Polar Engineers Confererence*. 3: 531-535. (1999).

Vishnuhotla, S., Falzarano, J. M. and Vakakis, A. A New Method to predict Vessel/Platform Critical Dynamics in a Realistic Seaway. *Philosophical Transactions of the Royal Society* 358: 1967-1981. (2000).

Vishnuhotla, S., Falzarano, J. M. and Vakakis, A. Storm survival of a tanker based FPSO in a realistic seaway. 10^{th} *International Society of Offshore and Polar Engineers Confererence*. 3: 391-395. (2000).

Vishnuhotla, S., Falzarano, J. M. and Vakakis, A. MOB platform nonlinear dynamics in a realistic seaway. *Journal of Offshore Mechanics and Arctic Engineering, Transactions of the ASME*. 124: 48-52. (2002).

Vishnuhotla, S., Falzarano, J. M. and Vakakis, A. Nonlinear dynamic analysis of ship capsizing in random waves. 14^{th} *International Society of Offshore and Polar Engineers Confererence*. 3: 479-484. (2002).

Vugts, J. H. *Hydrodynamic Forces and Ship Motion in Waves*, Ph.D. Dissertation at The Technical University of Delft, Ship Building Department, Delft. (1970).

Wiggins, S. *Introduction to Applied Nonlinear Dynamical Systems and Chaos*. Springer-Verlag. (1990).

Wolfram, J. Risk of capsize and loss of stability. *Risk and Reliability in Marine Technology*. C. Guedes-Soares (Editor), Balkema.A.A. 137-148. (1998).

Yamanouchi, Y. A Review of Statistical Studies of Seakeeping Qualities. *The Tenth David W. Taylor Lectures*. DTRC, Bethesda. (1986).

Zhang, F. and Falzarano, J. MDOF Global Transient Ship Rolling Motion: Large Amplitude Forcing. *Stochastic Dynamics and Reliability of Nonlinear Ocean Systems, ASME* WAM, September. (1994).

VITA

Srinivas Vishnubhotla was born in Hyderabad, India, and after receiving his early education from Hyderabad Public School - Ramanthapur, he obtained his high school diploma from St. Mary's Junior College (Hyderabad, India) in 1989. He graduated with honors with a degree in Bachelor of Science, Engineering, in Naval Architecture from the Indian Institute of Technology, Kharagpur, India in 1993. He was a graduate research assistant while enrolled in the Masters program in the School of Naval Architecture and Marine Engineering, University of New Orleans (UNO) from the Spring of 1994 till the Summer of 1997. The same year, shortly after passing the Ph.D qualifiers in Engineering and Applied Science in UNO, he went to work in the offshore industry first for Friede and Goldman Ltd (till November 2000) and then for Transocean Deepwater Drilling, offering his professional services from August 1997 till September 2003. During this time he also graduated from UNO with a degree in Master of Science in Engineering, with a concentration in Naval Architecture and Marine Engineering, in December 1998 and passed his General Exam for his Doctoral studies in March 2001. He came back to UNO in Spring 2004 as a Doctoral research assistant under the supervision of Dr. Jeffrey Falzarano to complete his Ph.D Dissertation and is currently a candidate for the Doctor of Philosophy in Engineering and Applied Science with a concentration in Naval Architecture and Marine Engineering at the University of New Orleans.